

## Fuel Level Estimation Methods

Master's thesis in Systems, Control and Mechatronics

Ellen Eskilsson and Alexander Örnescans



MASTER'S THESIS 2018:

Ellen Eskilsson, Alexander Örnescans



**CHALMERS**  
UNIVERSITY OF TECHNOLOGY

Department of Electrical Engineering  
CHALMERS UNIVERSITY OF TECHNOLOGY  
Gothenburg, Sweden 2018

Fuel Level Estimation Methods  
ELLEN ESKILSSON and ALEXANDER ÖRNESKANS

© ELLEN ESKILSSON and ALEXANDER ÖRNESKANS, 2018.

Supervisor: Aid Mujanovic and Andréas Olsson, Volvo Car Corporation  
Examiner: Balázs Adam Kulcsár, Associate Professor in the Automatic control  
research group at Chalmers University of Technology

Master's Thesis 2018:  
Department of Electrical Engineering  
Chalmers University of Technology  
SE-412 96 Gothenburg  
Telephone +46 703602289

Cover: Joint probability of two random variables. The relationship between two  
random variables will often tell how strongly they depend on each other and therefore  
plays a significant role for estimation and prediction.

Typeset in L<sup>A</sup>T<sub>E</sub>X  
Gothenburg, Sweden 2018

## Abstract

Being able to rely on the fuel level estimation is important for the driving experience. However unprocessed fuel level signals are highly noisy and therefore misleading. To ensure a good and predictable driving experience it is important to process the fuel level signals. The way this thesis has tackled this problem is by comparing and evaluating different model based estimation methods.

The estimation algorithms were designed based on a saddle type tank developed by Volvo Car Corporation. The fuel level sensor consists of a floater arm and can only detect fuel levels within its physical reach. The tank size can deviate from the standard volume and it will affect the measurement. Acceleration, angular orientation and fuel consumption are all factors related to fuel level estimation and therefore their relationship to the estimation problem is investigated.

An experiment was devised to investigate the relationship between angular orientation, fuel volume and fuel level readings. ARX based models were made including angular orientation. The relationship was concluded to be non-linear, since the magnitude of the fuel displacement depend on both current volume and angle orientation.

The Kalman,  $\mathcal{H}_\infty$ , Particle and Recursive Least Squares filters were compared. The Kalman and RLS filters had the most desirable traits and were therefore further developed.

Both Kalman and RLS resulted in smooth estimates on the driving cycles tested. The Kalman filter provided a steadier estimate and could be easily tuned for faster convergence to zero. The Kalman filter can easily be changed to accommodate parametric uncertainties which improve its robust qualities. The RLS method was considered more robust towards tank variation and tank ageing.

Keywords: Fuel volume estimation, Kalman,  $\mathcal{H}_\infty$ , Particle Filter, Recursive Least Squares



## Acknowledgements

This thesis was made in cooperation between Volvo Car Corporation, Chalmers University of Technology and Luleå University. We would therefore like to thank all three parties for making this thesis possible.

Firstly we would like to thank our Volvo supervisors Aid Mujanovic and Andréas Olsson, whom have given great advice and support throughout the spring. We would also like to express a large thank you our academic supervisors, Balázs Adam Kulcsár and Damiano Varagnolo, for continuously steering us in right directions. Thirdly we would like to thank everyone at VCC for making us feel welcome and showing us different interesting aspects of the company. A special thanks to Jonas Eklund och Rickard Kreuger for providing us of 3D rendered images of the fuel tank. We would also like to thank Niklas Klevendal, who both helped us collect data and gave us data that became vital for our project. We would also like to thank everyone at the EVAP garage, Krister Blom and Rickard Magnusson who helped us greatly with the experiment. Also a large thank you to Chrisofer Karlberg, who took great care of us thesis workers. Lastly we would like to thank everyone at VCC again for brightening up our time during the thesis. It has been a remarkable experience.

Ellen Eskilsson and Alexander Örnescans, Gothenburg, June 2018



# Contents

<b>List of Figures</b>	<b>xi</b>
<b>List of Tables</b>	<b>xiv</b>
<b>1 Introduction</b>	<b>1</b>
1.1 Background . . . . .	1
1.1.1 Problem description . . . . .	1
1.1.2 Motivation . . . . .	2
1.2 Research questions . . . . .	2
1.3 Aim . . . . .	2
1.4 Scope and limitations . . . . .	3
1.5 Outline . . . . .	3
<b>2 Theory and Method</b>	<b>4</b>
2.1 System . . . . .	4
2.1.1 Fuel tank . . . . .	4
2.1.2 Fuel level sensor . . . . .	5
2.1.3 Signals . . . . .	6
2.1.3.1 Fuel consumption . . . . .	7
2.1.4 Disturbances . . . . .	7
2.1.5 Orientation . . . . .	7
2.2 Modelling . . . . .	9
2.2.1 Modelling approaches . . . . .	9
2.2.2 System Identification . . . . .	9
2.2.2.1 ARX . . . . .	9
2.3 Filters . . . . .	9
2.3.1 Kalman Filter . . . . .	10
2.3.2 $\mathcal{H}_\infty$ Filter . . . . .	10
2.3.3 Particle filter . . . . .	11
2.3.4 Recursive Least Squares . . . . .	12
2.4 Quality of an estimator . . . . .	13
2.4.1 Mean squared error . . . . .	13
2.4.2 Variance Accounted For . . . . .	13
2.4.3 Standard Deviation . . . . .	14
2.4.4 Robustness . . . . .	14
2.5 Relationship between angle and fuel readings . . . . .	14

2.5.1	Hypothesis . . . . .	14
2.5.2	Experimental setup . . . . .	14
2.5.3	Experimental procedure . . . . .	15
<b>3</b>	<b>Implementation</b>	<b>17</b>
3.1	Model estimation . . . . .	17
3.1.1	Covariance analysis . . . . .	17
3.1.2	State transition model . . . . .	18
3.1.3	Measurement model . . . . .	19
3.1.3.1	Fuel displacement due to angle variations . . . . .	19
3.1.4	Final state space model . . . . .	22
3.1.4.1	Complex model . . . . .	22
3.1.4.2	Simple model . . . . .	23
3.1.5	Properties of the state space models . . . . .	23
3.2	Recursive Least Squares . . . . .	24
3.2.1	Fuel displacement due to acceleration . . . . .	24
3.2.2	RLS model formulation . . . . .	25
3.2.3	Robustness . . . . .	26
3.3	Filters . . . . .	26
3.3.1	Steady state Kalman and complimentary filter . . . . .	27
3.4	Comparison of filter structures . . . . .	27
3.4.1	Convergence . . . . .	27
3.4.2	Online refuel detection . . . . .	28
3.4.3	Detect offline refuelling . . . . .	29
3.4.4	Large angles . . . . .	30
3.4.5	Computational power . . . . .	32
3.4.5.1	Running time . . . . .	33
3.4.6	Conclusion of filter structure comparison . . . . .	33
3.5	Final Filters . . . . .	34
3.5.1	Online refuelling detection . . . . .	34
3.5.2	Offline refuelling detection . . . . .	34
3.5.3	Low fuel levels . . . . .	34
3.6	Filter evaluation . . . . .	35
<b>4</b>	<b>Discussion</b>	<b>39</b>
4.1	Filter evaluation . . . . .	39
4.1.1	Evaluation uncertainties . . . . .	39
4.1.2	Filter behaviour . . . . .	39
4.2	Motivation of research methodology . . . . .	40
4.3	Kalman frequency domain behaviour . . . . .	40
4.4	Future Development . . . . .	42
4.4.1	State detection . . . . .	43
4.4.2	The fuel consumption signal . . . . .	43
4.4.3	Adding a tank lid state to the network . . . . .	43
4.4.4	Implementation of angle logic . . . . .	44
4.4.5	Future evaluation . . . . .	44

<b>5 Conclusion</b>	<b>45</b>
<b>Bibliography</b>	<b>45</b>
<b>A Measurement instruments</b>	<b>I</b>
A.1 Cables . . . . .	I
A.2 Inertial Measurement Unit . . . . .	II
<b>B Measuring the resistance of the resistor cards in the tank</b>	<b>III</b>

# List of Figures

2.1	Two illustrations of a 71 litre fuel tank used within this thesis. Sub-figure a has stationary fuel and b has sloshing fuel. The tank is a saddle tank and is divided into one active and one passive chamber. The active side is the chamber to the right in both figures. [1] . . . . .	5
2.2	A fuel pump with a fuel level sensor. The resistor card, the arm and the floater is marked in the figure. The resistor card is attached to the fuel pump, which is the large white container. . . . .	6
2.3	A diagram of a car that describes the rotational axis such as yaw, pitch and roll. [2] . . . . .	8
2.4	Tank used in the data collection while placed on the tilt rig is seen to the left. To the right is the top of the pump shown together with the connection. . . . .	15
3.1	Correlation between angle and fuel level reading, depending on the total volume in the tank. A value with magnitude close to 1 indicate a strong relationship. . . . .	19
3.2	How the read values of volume change as the roll angle is varied. The measurements are plotted with a blue cross. A linear fitting is shown as a solid red line. . . . .	20
3.3	Coefficients $A(V)$ and $C(V)$ in the linear fitting $\Delta V = A(V)\Delta\theta_{Roll} + C(V)$ are functions of the total volume, $V$ . This figure shows the two coefficients the total volume vary from 5 litres to a full tank of 71 litre. The roll angle is varied. . . . .	21
3.4	Coefficients $A(V)$ and $C(V)$ to the linear model fitted $\Delta V = A(V)\Delta\theta_{Pitch} + C(V)$ . They change as a function of the total volume, $V$ . The coefficients are shown as the total volume vary from 5 litre to a full tank of 71 litre. The pitch angle is varied. . . . .	21
3.5	Two detrended signals, fuel level measurements and lateral acceleration. The correlation coefficient between the signals is -0.2138. The continuous line is the measured fuel level whilst the dashed line is measured lateral acceleration . . . . .	24
3.6	The graph shows two detrended signals. The correlation coefficient between the signals is -0.3280. . . . .	25

3.7	Fuel level estimations as the tank is refuelled. Subfigure 3.7a shows Kalman filter based on the simple model, the complex model as well as the steady state Kalman. Subfigure 3.7b shows the particle filter, $\mathcal{H}_\infty$ and the RLS filter. . . . .	29
3.8	Fuel level estimate as the vehicle is turned off around, refuelled and then turned on. . . . .	30
3.9	The raw volume readings together with Kalman and $\mathcal{H}_\infty$ estimates as the car is driven into a tilted position. The car stands in the tilted position in approximately 5 minutes before driven down to flat surface. . . . .	31
3.10	The raw volume readings together with RLS and PF estimates as the car is driven into a tilted position. The car stands in the tilted position in approximately 5 minutes before driven down to flat surface. . . . .	32
3.11	The raw volume readings together with Kalman and $\mathcal{H}_\infty$ in a and RLS and PF estimates in b as the car is driven into a tilted position. The car stands in the tilted position in both roll and pitch and is in the position for approximately 5 minutes before driven down to flat surface. . . . .	32
3.12	Kalman and RLS estimates based on a drive from a full to an empty tank. Both estimators give a stable value throughout the drive. Kalman estimator have a value closer to zero as the car stops. . . . .	35
3.13	Raw values for a drive cycle from full tank to engine stall. The cycle ends with an online refuel. Both Kalman and RLS estimate the empty tank closely before the engine stalls. . . . .	36
3.14	Raw volume measurements as a car is driven to engine stop due to missing fuel. Both the Kalman and the RLS estimation estimate zero volume before the stall. . . . .	36
3.15	A driving cycle including hosing, driving to empty, refuelling to full tank and finally normal driving. The Kalman and the RLS both indicate zero before the engine stop, with Kalman estimating an empty tank first. . . . .	37
3.16	Driving from a full 71 litre tank. The Kalman filter and the RLS filter estimate different fuel levels, with Kalman estimating a lower volume. . . . .	37
3.17	Diving from circa one third full tank to empty twice, followed by one sixth full to empty. The first refuelling is done in steps. The Kalman estimate zero remaining fuel before the RLS does for both engine stops. . . . .	38
4.1	Bode plots for the transfer functions between the input fuel consumption and level estimate in a, fuel level measurement and estimate in b. The consumption to estimate act as an all pass filter, and the measurement to estimate act as a low pass filters. . . . .	41
4.2	Singular value depending on frequency for different tunings. The tuning used in the final Kalman, $\rho = 10^{10}$ is a solid black line. 10 and 100 times larger and smaller $\rho$ is also shown. . . . .	42

## List of Figures

---

- A.1 Image a is a cable that connects to the m-sense sensor as well as the male BNC connectors on image b . . . . . I
- B.1 The measurement circuit with a 5 volt voltage source. Measurement is done across the known resistor as seen by the voltage meter . . . . III

# List of Tables

3.1	Correlation coefficients for named signals and the fuel level sensor value. . . . .	18
3.2	Time needed before filter has converged. Convergence time is showed in minutes. . . . .	28
3.3	Mean square error, variance accounted for and covariance for the different filters compared to the raw signal as new fuel is inserted. . . . .	29
3.4	Running time of various filter algorithms under one iteration . . . . .	33

Abbreviations used in the report and their meanings in alphabetical order.

Abbreviation	Meaning
ARX	Auro- Regressive with eXogenous input
Cov	Covariance
IMU	Inertial Measurement Unit
KF	Kalman Filter
LS	Least Square
MSE	Mean Squared Error
PF	Particle Filter
RLS	Recursive Least Squares
RPM	Revolutions Per Minute
STD	Standard Deviation
SYSID	System Identification
VAF	Variance Accounted For
VCC	Volvo Car Corporation

# 1

## Introduction

This Master thesis has been conducted at Volvo Car Corporation VCC, in Gothenburg. It was conducted within the departments of Fuel Distribution and Driver Information. VCC is a Swedish automotive company that produces premium automobiles and is owned by Geely Holding Group.

### 1.1 Background

The fuel level is one of the corner stones when a driver plans the driving. Knowing when to refuel is important, and basing the plan on inaccurate information may have big consequences. The fuel level measurements are noisy and may be misleading due to the movement of the fuel. It is therefore necessary to process the measurements before displaying the information to the driver.

The current method in which the fuel level is displayed emphasises on stability, the ability to tell the driver that fuel level is zero when the tank is empty and detecting when refuelling is done. Such information helps with trip planning and distance to empty predictions. However, during certain situations the fuel level estimation may be slightly inaccurate. It is therefore interesting to investigate alternative methods.

#### 1.1.1 Problem description

The fuel level sensor of concern is a variable resistor that is attached to a arm equipped with a buoyant floater. The position in which the arm is in will determine the resistance of the variable resistor. This resistance is thus proportional to the fuel levels and can therefore give a fuel level reading. However the possible resistances in which the variable resistor can achieve are done in discrete steps, therefore the sensor has a certain measurement resolution. It is also important to note at two thresholds, dead-zones, the fuel level sensor cannot acquire accurate fuel level information. This is because there is a physical limitation in which the arm can be positioned in. [3]

However reading fuel levels is not as simple as reading the raw sensor values. There are sources of disturbances and uncertainties that affect the precision and accuracy of the measured fuel levels.

Mechanical disturbances or process noise affect the measured fuel levels. The liquid in the tank may produce a sloshing phenomena in the tank as the car accelerates or decelerates. The angular orientation of the car also changes the displacement of

the fluid in the tank. Fluid motion and its displacement in the tank will be influenced by the actual fluid volume. [4] These disturbances affect the position of the floater arm and therefore changes the measured fuel level readings.

The tank comes with a standardised mathematical model that is a look up table, that transforms resistance into fuel level volumes. A look up table is made for a specific tank type, size and may not be an exact representation of all tanks of that type. The making of a tank table is also exposed to measurement noise.

The sensor itself may also be noisy which is yet another factor that influences fuel level readings.

Many traditional methods uses a frequency domain approach to solve the problem. However there are many other alternative approaches to solving this estimation problem and some of these alternatives will be investigated in this thesis.

### 1.1.2 Motivation

The issues discussed in Section 1.1.1 can cause instabilities in fuel level readings. These issues may cause several problems to occur which may diminish the overall driving experience.

It is important for drivers to know how much fuel is in the car as this helps with distance to empty prediction. Such prediction help with trip planning, when to refuel and how to drive. Trip planning becomes difficult when fuel level readings are inconsistent or inaccurate. Since there are deviations in tank geometry the fuel level reading can potentially be positive when in reality it is zero. This could leave the driver stranded on a road with no fuel. Fuel level readings can be inconsistent when the vehicle is at an angle, which could leave the driver to believe that he or she has more or less fuel than in reality. Such problems can be solved through filtration strategies in software and in turn improve the driving experience.

Since there are no definitive answers to digital fuel level estimation it is important to look at different strategies that provide a robust fuel level estimation. The reason for a robust method is that there are deviations in tank volumes, as well as modelling uncertainties that govern fuel level prediction. There are cases that bring up non-linear behaviour such as slosh, refuelling online and offline that the estimator needs to take into account.

## 1.2 Research questions

The three research questions this thesis aims to answer is:

- How to make the fuel level estimation more reliable?
- What estimation methods can provide a sufficient fuel level estimation?
- What signals can be used in the estimation?

## 1.3 Aim

The objective of this master thesis is to evaluate different filtration strategies that provide a robust estimation of the fuel level. This will be done by:

- Applying different modelling techniques that model the fuel level dynamics.
- Construct model based fuel level estimators.
- Comparing and contrast different model based estimation strategies.

### 1.4 Scope and limitations

The algorithms that govern fuel level estimation, will be developed based on the fuel system present in the cars currently manufactured by VCC. Two different fuel tank shapes are of use in cars produced by VCC, but only the saddle tank type will be considered during filter development. Conditions where fuel boils or where the car overheats will not be considered in the filter development. Neither crashes or situations where the car is flipped upside down, for example after a large collision, will be covered. In other terms what will be mainly considered are general driving scenarios.

Conditions that will be considered in the filter development are

- Driving from full to empty tank.
- Refuelling online and offline.
- Inclined parking.
- Driving under heavy acceleration.
- City and highway driving.

### 1.5 Outline

This report is divided into five chapters. In Chapter 2 is theory behind the system, the modelling and the different estimation algorithms presented. The methodology behind an experiment is presented as well. Chapter 3 contains the implementation of the theory and the result from the experiment. It describes the modelling, the implementation of the model and the comparison of different algorithms. In Chapter 4 is the method and the result discussed. Chapter 5 contains an conclusion.

# 2

## Theory and Method

This chapter describes the system used, followed by information about the principals behind modelling and different filter design strategies.

### 2.1 System

This section describes the system that will be investigated within the thesis. The signals of interests, tank architecture and disturbances that influence fuel level readings will also be described.

#### 2.1.1 Fuel tank

The fuel tank acts as a storage unit for fuel and when needed the pump inside the tank sends fuel to the engine. The tank can come in various sizes and forms, however filter development will be focusing on a saddle tank. Two illustrations of a saddle tank are showed in Figure 2.4, one in which the fluid is still and one in which the fuel is sloshing. A saddle tank has two chambers, one active and one passive. The two chambers are separated by a low wall which allows fuel to move from one side to the other. A pump transfers fuel from the passive to the active side. Each of the two chambers are fitted with a level sensor mirrored from each other. They are placed mirrored from each other, to compensate for the change in fluid displacement as a result from the car being tilted. [5]

The production of plastic tanks that are of concern in this thesis are done through blow moulding. This process is not fully precise and therefore the tanks that are made can deviate in size with reference to the desired tank volume. [3]

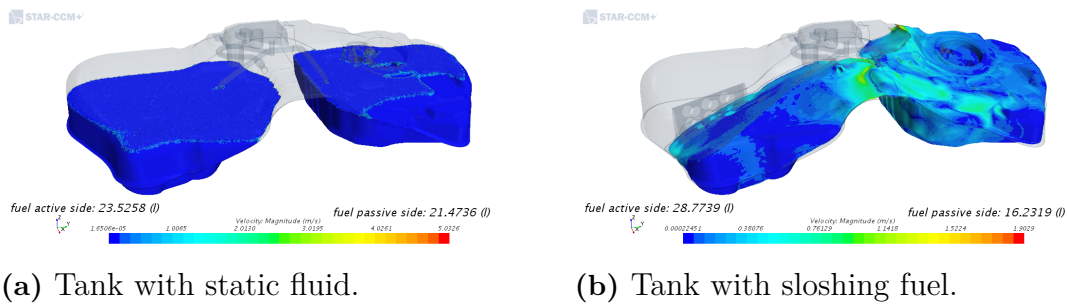


**Figure 2.1:** Two illustrations of a 71 litre fuel tank used within this thesis. Sub-figure a has stationary fuel and b has sloshing fuel. The tank is a saddle tank and is divided into one active and one passive chamber. The active side is the chamber to the right in both figures. [1]

### 2.1.2 Fuel level sensor

There are multiple ways to measure fuel levels in a fuel tank. One of the most popular and economically viable solutions within the automotive industry is a variable resistor attached to an arm with a floater. Figure 2.2 shows a floater arm attached to the fuel pump. The floater ensures that the arm can be either raised or lowered depending on the amount of fuel in the tank. Raising the arm decreases the resistance of the variable resistor and lowering the arm increases the resistance. The resistance changes in discrete steps which affects the precision of measured fuel levels. There is also a min and max position the arm can be in and therefore, a min and max resistance that can be achieved. This affects max fuel level readings, since liquid above the maximum raised position of the arm cannot be detected. Once a known voltage is applied to the variable resistor it is possible to measure the voltage drop with changes in resistance. This voltage signal can be directly mapped to the position of the arm and thus the amount of liquid in the tank. The measurement resolution of the sensor that will be investigated is 0.2 litres. This mapping is currently done through a look-up table.

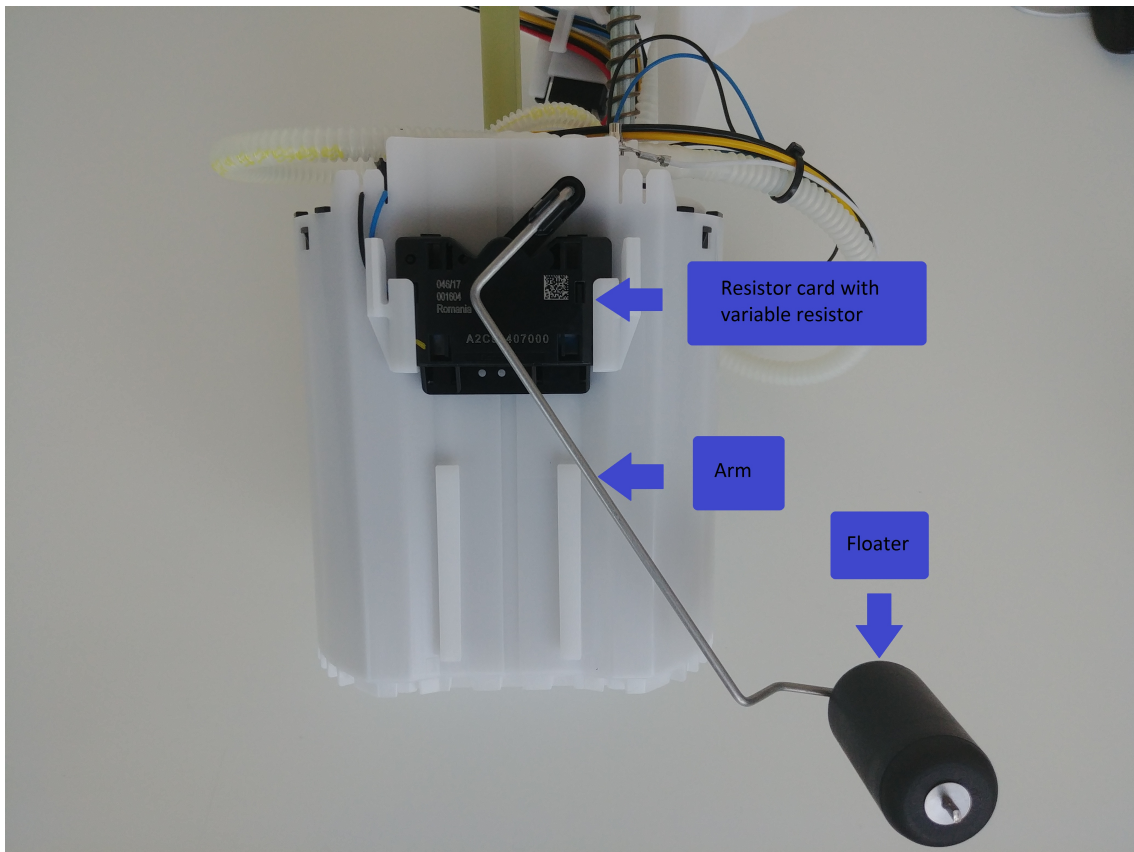


**Figure 2.2:** A fuel pump with a fuel level sensor. The resistor card, the arm and the floater is marked in the figure. The resistor card is attached to the fuel pump, which is the large white container.

### 2.1.3 Signals

The identification of a parametric model depends on the available signals on the Flexray network. FlexRay is a deterministic communications protocol used in the cars produced by VCC. [6]

This subsection presents some of the available signals used.

- Volume measurements.  
Subsection 2.1.2 describes the volume measured by two floater arms. Both the raw resistance values and the translated volume values are available.
- Usage mode status.  
A signal containing information on state of the car, for example when in the driving or inactive state.
- Vertical, lateral and longitudinal acceleration.  
The cars acceleration in three directions are available on the network. They all originate from accelerometers.
- Angular orientation in pitch, yaw and roll.  
The car orientation is described through angles, given in radians.
- Fuel consumption.

### 2.1.3.1 Fuel consumption

The amount of fuel available in the tank is directly linked to how much fuel is consumed over a period of time. The consumed fuel is estimated using injection cycles. By knowing how long fuel is injected into the cylinders in the motor of the vehicle, it is possible to estimate the instantaneous loss of fuel. Heating also consumes fuel and therefore is also included in the fuel consumption signal. However this method is not fully accurate and its maximum uncertainty is approximately X%. It is worth noting that this thesis does not focus on fuel consumption prediction however it is worth discussing about it for future work.

### 2.1.4 Disturbances

The liquid in the fuel tank has the freedom to move once there is space for such motion. Such motion changes the overall displaced liquid in the tank and are caused by certain factors. The way that the fuel is displaced in the tank will also determine how the fuel level sensor arm is positioned, which in turn affects the read fuel levels.

Sloshing is the motion of a fluid inside a object, in this case a fuel tank. The phenomena can either be linear or non-linear and in this thesis both cases are prevalent. This sloshing phenomena displaces the liquid in the tank differently in time and therefore influences the position of the floater arm which in turn disturbs fuel level readings. Such sloshing occurs when the vehicle accelerates and decelerates. The fuel movement is also dependent on how rapid the acceleration changes. [4]

The resistance of the resistor card in fuel level sensor is mapped to a volume through a look-up-table. As mentioned tank sizes can vary and therefore this mapping may be less accurate for different individual tanks.

Angular orientation will decide how the fluid is displaced in the tank. The fuel level sensor is also effected, since the floater arm floats on the fluid. As the fluid is displaced differently the readings may indicate an increase or decrease in fuel levels.

### 2.1.5 Orientation

Angular orientation is a way to describe the orientation of a body in the space it occupies. That is the amount of rotation that is required to move the object to a new position. In this case three axis are used to describe the orientation of the cars. Typically the terms roll, yaw, and pitch are used to describe these three axis.

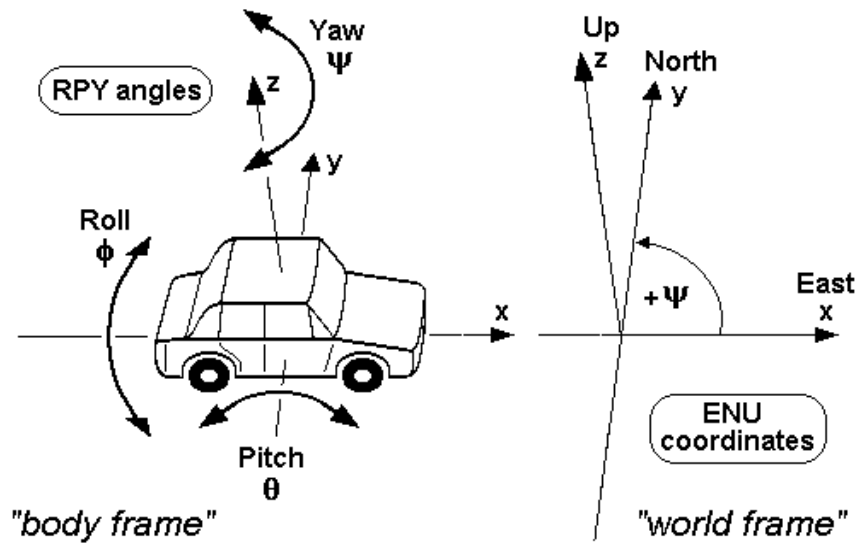


**Figure 2.3:** A diagram of a car that describes the rotational axis such as yaw, pitch and roll. [2]

An illustration of the roll, pitch and yaw is shown in Figure 2.3. Roll is found at the centre of gravity around the vehicle. This rotation is directed forward towards the grill of the car. If there is change in roll then the left wheels will be lifted, the right wheels will be lowered and vice-versa.

Yaw is found at the centre of gravity around the vehicle. This rotation is directed toward the top of the vehicle. If change in yaw were to happen then the nose of the vehicle would change in direction. In a car yaw can be changed by moving forward or backwards and simultaneously changing directions with the steering wheel.

Pitch is found at the centre of gravity around the vehicle. This rotation is directed towards the left of the vehicle. Positive changes in pitch will raise the front of the car up, lower the trunk and vice-versa. [7]

## 2.2 Modelling

Modelling and approximating reality is important within science and engineering as it helps understanding the properties and behaviours of a system. With such knowledge it is possible to predict the future behaviour of the systems and rule out outliers. It is therefore desirable to use a model based approach while filtering a signal. Proper or strictly proper, causal models are considered. Some of these modelling approaches are discussed in the subsection below.

### 2.2.1 Modelling approaches

Methods to model systems can be divided into three different approaches: white-, black- and grey-box models. White-box models are completely based on theory. Black-box models uses no prior knowledge about the system and is only based on the available data. Grey-box models have some knowledge about the system but some parameters or relationships remain unknown. It therefore uses both knowledge about the physical model and available data. [8]

### 2.2.2 System Identification

System identification is a technique to build a model representation of a dynamical system through measurements and methods in statistics. It can be used both in grey- and black-box modelling. System identification typically uses a predetermined model structure with unknown coefficients. These coefficients are found through the minimisation of the difference between the estimation and the actual measurement with respect to a cost function. [9]

#### 2.2.2.1 ARX

The Auto-Regressive with eXogenous input model ARX, is a simple approach to modelling. It maps a certain output as a combination of delayed outputs, inputs and single varying error in its prediction. The model assumes the form:

$$\begin{aligned} y(k) + a_1y(k-1) + \dots + a_{n_a}y(k-n_a) = \\ = b_{1_b}u(k-1) + \dots + b_{n_b}u(k-n_b) + e(k) \end{aligned} \tag{2.1}$$

where  $y$  is the set of outputs,  $u$  the set of inputs and  $e(t)$  the innovation term. The coefficients  $a_i$  and  $b_i$  are chosen to minimise a cost function. [9] The ARX model is of interest as it is a model that is easily implemented and has a separate innovation term.

## 2.3 Filters

This section describes different filtering algorithms. The filters described in this section are model based filters.

### 2.3.1 Kalman Filter

The Kalman filter is an optimal filter as long as the following criteria are met. Optimality is regarding state estimation error covariance minimisation.

- The system dynamics are linear, see Equation 2.2, and perfectly matches the real system.
- Process noise and measurement noise are un-correlated and zero-mean white noise.
- The system dynamics are observable and detectable.

However cases where the noise is Gaussian yields an exact conditional probability estimate.

In Equation 2.2,  $x(k)$  is the state vector at time instance  $k$ ,  $u$  is the input,  $w$  is the process noise,  $v$  is the measurement noise and  $y$  is the measured variable. Describing a system in this form is called state space representation. [10]

$$\begin{aligned}x(k) &= Ax(k-1) + Bu(k) + w(k) \\y(k) &= Cx(k) + v(k)\end{aligned}\tag{2.2}$$

The first equation is called the state transition model, and describes what the state is predicted to be in the next time instance. The second equation is called measurement model, and relates measurements to the states.

The Kalman filter has two stages, the prediction and the update step. At the prediction step, the state vector and co-variance matrix at the time instance  $k+1$  is predicted with the use of the state-transition matrix. It is shown in Equation 2.3. Predicted state value is denoted  $x(k|k-1)$ , which means that it is the state value at time instance  $k$  based on all the measurements made up to instance  $k-1$ . The same applies for the co-variance matrix  $P(k|k-1)$ .

$$\begin{aligned}\hat{x}(k|k-1) &= A\hat{x}(k-1|k-1) + Bu(k) \\P(k|k-1) &= AP(k-1|k-1)A^T + Q\end{aligned}\tag{2.3}$$

In the update step shown in Equation 2.4, the new state is given by the previous state plus a gain multiplied by the predicted state and the measured state. The Kalman gain,  $K(k)$ , is used to update the state value to fit both the predicted and the measured value. [11]

$$\begin{aligned}K(k) &= P(k|k-1)C^T(CP(k|k-1)C^T + R)^{-1} \\ \hat{x}(k|k) &= \hat{x}(k|k-1) + K(k)(y(k) - C\hat{x}(k|k-1)) \\ P(k|k) &= (I - K(k)C)P(k|k-1)(I - K(k)C)^T + K(k) \cdot R \cdot K(k)^T\end{aligned}\tag{2.4}$$

It is important to note that the co-variance matrix converges to the optimal algebraic Riccati solution after some iterations.

### 2.3.2 $\mathcal{H}_\infty$ Filter

The  $\mathcal{H}_\infty$  approach is similar to the Kalman filter, but differs in the minimisation problem. Kalman filters try to minimise the covariance of the estimation error

and is a special case of the  $\mathcal{H}_2$  filter. [12] However the  $\mathcal{H}_\infty$  approach formulates the estimation problem in a different way. It quantifies modelling uncertainties, as a maximal error and tries to guarantee convergence of the estimation in these conditions. This makes the filtering approach robust to modelling uncertainties and all types of noise. In other words the  $\mathcal{H}_\infty$  approach tries to minimise the worst case estimation error, such that  $\sup(\frac{\|e\|_2}{\|d\|_2}) < \gamma$ , where  $e$  and  $d$  are the estimation error and the process and sensor noise respectively. The variable  $\gamma$  is a tuning parameter and is the worst case amplification, [13].

One iteration of the  $\mathcal{H}_\infty$  estimation algorithm can be expressed as:

$$\begin{aligned} L(k) &= \left( I - QP(k)\gamma + C^T V^{-1} C P(k) \right)^{-1} \\ K(k) &= AP(k)L(k)C^T V^{-1} \\ \hat{x}(k+1) &= A\hat{x}(k) + Bu(k) + K(k)(y(k) - C\hat{x}(k)) \\ P_{k+1} &= AP(k)L(k)A^T + W \end{aligned} \tag{2.5}$$

Where  $I$  is an identity matrix,  $Q$  is a weighting parameter,  $P(k)$  is the co-variance matrix and  $V$  and  $W$  are tuning parameters that model the system noise properties.  $K(k)$  is the  $\mathcal{H}_\infty$  gain. [14]

The cost function of the  $\mathcal{H}_\infty$  filter is essentially the ratio between  $Q$  divided by  $V$  and  $W$ , which is the ratio between  $Q$  over process disturbances and sensor noise. These two disturbances are usually modelled as a type of sensitivity and complementary sensitivity function that describes the upper bound of each respective signal. It is important to note that gamma has to be chosen such that  $P$  has eigenvalues less than one. This constraint will determine whether there is a solution to the  $\mathcal{H}_\infty$  problem. [15]

### 2.3.3 Particle filter

Particle filters, PF, has the ability to estimate highly nonlinear systems under the right circumstances. It approximates the distribution of a variable using particles. A state space model is still required, but is denoted as a probability distribution. The measurement model can hence be denoted  $p(x(k)|x(k-1),y(k))$ , which is the probability of  $x(k)$  given  $x(k-1)$  and  $y(k)$ .

PF uses the sequential importance sampling algorithm. It uses  $N$  particles, which is initially distributed as the initial distribution. Each particle,  $x^{(i)}$ , is updated at each time instance  $k$  according to Equation 2.6.

$$x(k)^{(i)} \sim q(x(k)|x(k-1)^{(i)},y(k)) \quad i = 1, \dots, N \tag{2.6}$$

The distribution  $q$  is called the importance density and can be chosen differently dependant on the current available signals and models. The common choice is however the distribution shown in Equation 2.7.

$$q(x(k)|x(k-1),y(k)) = p(x(k)|x(k-1)) \tag{2.7}$$

Each weight is also computed at every time instance  $k$ :

$$w_{(k)}^i \propto w_{k-1}^{(i)} \frac{p(y(k)|x(k)^{(i)})p(x(k)^{(i)}|x(k-1)^{(i)})}{q(x(k)^{(i)}|x(k-1)^{(i)},y(k))} \tag{2.8}$$

The weights are then normalised.

Finally, the probability for the new state value is calculated. [16]

$$p(x(k)|y(1:k)) \approx \sum_{i=1}^N w_k^{(i)} \delta(x(k) - x(k)^{(i)}) \quad (2.9)$$

One common problem is degeneracy. That means that eventually all but one particle will have a weight close to zero. Re-sampling can be used to avoid this problem. The first step of re-sampling is to draw  $N$  samples with replacement from the set of particles at the current time instance. The probability of picking a particle is the same as the corresponding weight. This new set replaces the old particle set and all weights are set to  $\frac{1}{N}$ . [17]

### 2.3.4 Recursive Least Squares

The physical system modelled may change over time. It can therefore be preferable to update the parameters of the model as the system dynamics evolves.

The Recursive Least Squares algorithm, RLS, is an online regression method that computes the parameters of a given model whilst minimising a linear weighted least squares problem. This is in contrast to the offline method where the solution of the parameters and total cost are found once over a finite data set. In essence the coefficient that govern the linear dynamics and the cost of the cost function are computed at every time a new data point is given to the algorithm by finding coefficients that minimise the cost.

$$\sum_{k=0}^N e^2(k) \lambda^{N-k} \quad (2.10)$$

Equation 2.10 demonstrates the weighted least squares cost function as a function of the coefficient vector. The objective is to minimise this cost online.  $N$  is the amount of samples and  $\lambda$  is the forgetting factor. The forgetting factor is often a scalar between 0.98 and 1, and in layman's terms the  $\lambda$  value tells how long in history the error cost should be remembered. By remembering and accumulating the error cost far back in history equates to a value close to 1. Making history less important equates to a value closer to 0.98. A higher value also leads to a robust estimation towards measurement noise, but will adapt slowly as the physical system changes.

The  $p$  last values of the state value are placed in the state vector:

$$\mathbf{x}(k) = \begin{bmatrix} x(k) \\ x(k-1) \\ \vdots \\ x(k-p) \end{bmatrix} \quad (2.11)$$

This is due to limit the memory demands on the algorithm, since using all the past value will make the problem grow with time.

$$\alpha(k) = d(k) - \mathbf{x}^T(k) \mathbf{w}(k-1) \quad (2.12)$$

The gain vector is denoted  $\mathbf{g}(n)$  and is calculated at every time instance according to Equation 2.13.

$$\mathbf{g}(k) = \mathbf{P}(k-1)\mathbf{x}(k) \left\{ \lambda + \mathbf{x}^T(k)\mathbf{P}(k-1)\mathbf{x}(k) \right\}^{-1} \quad (2.13)$$

Where  $\mathbf{P}$  is calculated according to Equation 2.14.

$$\mathbf{P}(k) = \lambda^{-1}\mathbf{P}(k-1) - \mathbf{g}(k)\mathbf{x}^T(k)\lambda^{-1}\mathbf{P}(k-1) \quad (2.14)$$

Finally the weight  $\mathbf{w}$  can be calculated. [18]

$$\mathbf{w}(k) = \mathbf{w}(k-1) + \alpha(k)\mathbf{g}(k) \quad (2.15)$$

It is important to note that the RLS filter uses the algebraic Riccati equation, similar to the Kalman filter.

## 2.4 Quality of an estimator

Determining whether an estimator is sufficient can be difficult, especially when no true state is available for comparison. There are however methods that help with the analysis of an estimator in terms of its estimation performance.

### 2.4.1 Mean squared error

Mean squared error, MSE, is a common measure of estimator accuracy. Computing the MSE is shown below

$$\text{MSE} = \frac{1}{n} \sum_{k=1}^n (Y(k) - \hat{Y}(k))^2. \quad (2.16)$$

where  $\hat{Y}_i$  is the predicted state at time step  $n$  and  $Y$  the measured variable. The MSE is always non negative due to the square. A value closer to zero indicates a good estimator. [19]

### 2.4.2 Variance Accounted For

Variance Accounted For, VAF, is another way of measuring the quality of a estimator. VAF explains how the variance of the original data set is related to the variance of the estimated data set. The variance of the estimated data set should be less than the original data set. The difference between the estimate,  $\hat{y}$ , and the measurement,  $y$ , is divided by the variance of the measurement. [20] VAF is calculated by implementing Equation 2.17.

$$\text{VAF}_k = \left( 1 - \frac{\text{var}(y(k) - \hat{y}(k))}{\text{var}(y(k))} \right) \cdot 100\% \quad (2.17)$$

A high VAF-value indicate a good estimate.

### 2.4.3 Standard Deviation

Standard deviation, STD, describes how far or dispersed the estimator is from the true value. A low STD indicates an even error over the data set, while a large STD indicates large variations. [21] It is calculated by:

$$STD = \sqrt{E[x - \mu_x]} \quad (2.18)$$

where  $\mu_x$  is the mean of  $x$  and  $E[\ ]$  is the expected value operator.

### 2.4.4 Robustness

A term that is used in this thesis to describe filters is robustness. A filter can be tuned to perform well for specific data sets. The parameters of a model can also be identified with a use of a specific data set, however in order to validate the models or filters other data sets need to be used. This will determine how robust the models or filters are to new scenarios. A model or filter is considered robust if the predictions behave as desired to new scenarios and circumstances.

## 2.5 Relationship between angle and fuel readings

This section explains the method in which data was gathered to study the relationship between tank volume readings versus roll, pitch and actual volume. The materials and lab setup that were used during the experiment are described in detail in Appendix A.

### 2.5.1 Hypothesis

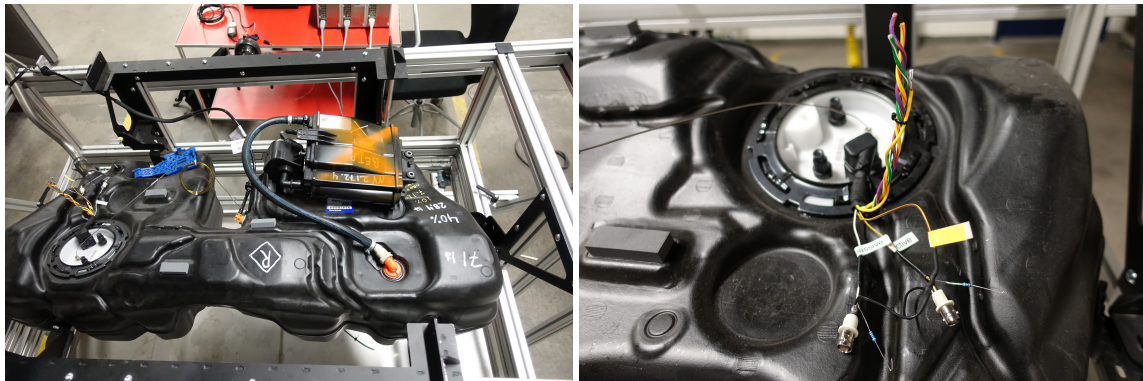
The idea behind this experiment was to capture the dynamics involved with how fuel level readings changed based on a change in angular orientation of the tank. These angles include pitch and roll. Yaw is not included as gravity does not act on the fluid in that axis.

As a result of different angular orientations the fluid in the tank will move and thus be displaced differently. Because of such change the floater arm in the tank will also be positioned differently, which will in turn change the resistance of the variable resistor, thus changing fuel level readings.

Thus the aim of this experiment is to capture how change in roll and pitch changes the fluid level readings over different sets of volumes.

### 2.5.2 Experimental setup

Before the experimental method can be explained in details it is important to first understand some of the equipment and materials used in the experiment.



(a) 71 litre tank

(b) Connection to pump

**Figure 2.4:** Tank used in the data collection while placed on the tilt rig is seen to the left. To the right is the top of the pump shown together with the connection.

The tank used was a saddle type and estimated to hold 71 litres of petrol from manufacturing specifications, however with a possibility of some deviation. It was attached to a tilting rig that allowed for variations in roll and pitch. The tank placed inside the tilt rig can be seen in Figure 2.4. These pitch and roll variations are done through rotating a circular lever by hand.

The level measurements were measured through the cables and resistors seen in Figure 2.4b. The angles were measured through a phone, which was placed on the middle top part of the tank. The time in which measurements start is dependant on when both the phone and level measurements are started. Two people are needed in order to start the devices simultaneously and because of such a factor the time vector of each respective measurement may be out of sync. To combat this issue, a separate sensor that measures angles, with less accuracy than the phone, is connected to the same network as the level measurements. The tank itself was placed in the tilt rig such that the rotation axis was in the middle cross section of the tank. Detailed description of the cables, power suppliers and other equipment can be found in Appendix A.

### 2.5.3 Experimental procedure

Once the tank is attached to the tilt rig and the angle measurement units are attached on to the top middle portion of the tank, the software is set to record at 50 Hz. The measurements of the tank volumes are started along with the sensors.

Once the equipment have been prepared the tank is first tilted very slowly in roll. The experiment always ends at the initial starting point in roll, i.e. 0 degrees. The procedure is then repeated but now for pitch. Pitch is varied slowly and always ends at 0 degrees.

5 litres of fuel are added to the tank with the use of a measuring jug. This procedure is repeated until the tank is full.

It was only possible to measure voltages with the equipment. However what is of interest is the resistance inside the resistor card of the fuel level sensor. This problem was solved by measuring the voltage drop over a known resistance. A more

## 2. Theory and Method

---

detailed explanation together with a circuit diagram and a derivation of how the resistance relate to the voltage drop can be seen in Appendix B.

# 3

## Implementation

In this chapter the theory and the result from the experiment described in Chapter 2 are implemented. Firstly is a model based on the angle experiment estimated, followed by a RLS based on the same experiment. The model is then implemented in different filter structures and compared with each other and the RLS. The two most successful filters are then developed further and finally evaluated.

### 3.1 Model estimation

This section describes the process of modelling fuel level dynamics. It results in two different state space models, one simple and one complex model, which are to be implemented in filter structures further on in this report.

#### 3.1.1 Covariance analysis

The initial stages of system identification requires the selection of signal or variables that affect the measured output. In this case this section presents the correlation coefficient between raw fuel level signals and signals describing the motion of the car.

The correlation coefficient,  $\rho$ , for two signal arrays  $A$  and  $B$  is calculated according to Equation 3.1.

$$\rho(A,B) = \frac{1}{N-1} \sum_{i=1}^N \left( \frac{A_i - \mu_A}{\sigma_A} \right) \left( \frac{B_i - \mu_B}{\sigma_B} \right) \quad (3.1)$$

where  $\mu$  is mean,  $\sigma$  is standard deviation and  $N$  is the amount of samples. The correlation coefficient is an indication on the linear dependency of two signal arrays. [22]

Correlation coefficients for a number of signals relative to fuel level readings are shown in Table 3.1. The coefficients are calculated based on a measurement where the car is driven from a full 50 litre tank to an empty tank. A 50 litre tank was used due to lack of available 70 litre data. Relationships between different signals should be similar between different tank sizes. Certain sections of a data set could yield higher or lower correlation coefficients. However this section covers the correlation between the whole data sets. A high absolute value indicates a strong linear relationship, while a small absolute value indicates a small relationship or a nonlinear one.

**Table 3.1:** Correlation coefficients for named signals and the fuel level sensor value.

Signal	Correlation
Fuel Consumption	-0.8347
Lateral acceleration	-0.3564
Velocity	0.2733
Roll	0.1513
Pitch	0.1281
Roll rate	0.0370
Longitudinal acceleration	-0.0244
Vertical acceleration	-0.0124

It is visible from Table 3.1 that fuel consumption has a negative correlation coefficient. This means that as fuel levels decreases there is an increase in fuel consumption, which is a reasonable trend. The absolute value of the correlation coefficient is largest among the signals investigated that indicate a strong linear relationship.

The two angles roll and pitch have correlation coefficients 0.15 respectively 0.13. The magnitude of these values are large enough for a linear relationship, however it is also possible that this relationship is not significant for certain data sets. The data used in Table 3.1 is from city and highway driving and no steep hills are included. The angles are therefore limited to small changes and it is reasonable that the effect on the fuel level readings is not large.

It is however not in these driving scenarios that the angle should be of interest. For example for a car parked in a tilted position, it would be possible to establish a stronger relationship with angles. [23] It is therefore still interesting to evaluate the angle's effect.

Vertical acceleration has a correlation coefficient close to zero and this could be indicative of a poor linear relationship to fuel level readings. Lateral acceleration on the other hand has a non-zero coefficient and its relationship should be looked into further.

It has also in a previous master thesis at VCC been concluded that longitudinal and lateral acceleration in some cases can have major impact on the fuel level readings. [23] It is therefore interesting to investigate longitudinal acceleration further, despite the low correlation.

### 3.1.2 State transition model

The theoretical change in fuel volume is the fuel consumed by the car. Thereby the current fuel level reading is the previous reading subtracted with the consumed volume of fuel. This claim is supported by the covariance analysis done in Section 3.1.1. The analysis concluded that there was a strong negative linear relationship between the fuel level reading and the consumed fuel. This can be expressed as a state transition model,

$$x(k+1) = x(k) - u(k) \quad (3.2)$$

where  $x_k$  is the fuel volume at instance  $k$  and  $u$  is the consumed fuel since the last time instance. The state transition model predicts the consecutive level, but does not relate the state to the measurement. The measured fuel level can be seen as a function of the fuel state and fuel displacement due to angular orientation. This function is called a measurement model.

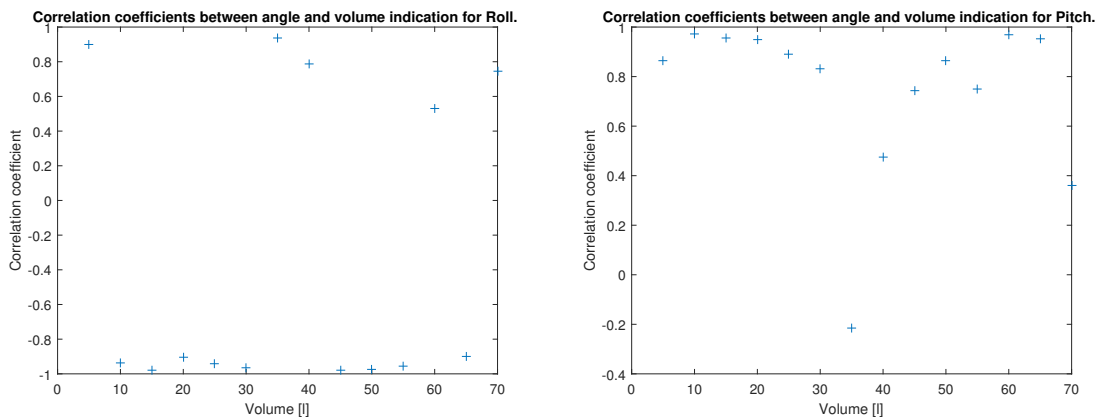
### 3.1.3 Measurement model

A measurement model is used to relate the measurements to the states. This section describes the modelling procedure and how angles, volume state and level measurements relate to each other.

#### 3.1.3.1 Fuel displacement due to angle variations

Logically, the fuel level reading will be most accurate when the car is horizontal. As the tank is tilted, the fuel reading error will increase due to the change in the fluid displacement. The execution of the experiment in which the tank is tilted was described in Section 2.5. Result of the experiment is presented in this section together with a parametric model based on the result.

Figure 3.1 shows the correlation between angular displacement and the fuel volume readings for the different tested volumes. Every fifth litre between 5 and 71 litre is tested. For the majority of the tested volumes, the correlation has a magnitude above 0.8, indicating a linear relationship between angle and volume displacement. The sign of the correlation coefficient vary, due to the placement of the sensor. It is however important to remember that a nonlinear function can behave piecewise linear for small angles, for examples sinus and tangens. The correlation is smaller for the total volumes 35 and 40 litres as the pitch angle is varied. This might come from the active side of the tank being full, making less room for volume displacements and therefore saturating the movement.



(a) Roll

(b) Pitch

**Figure 3.1:** Correlation between angle and fuel level reading, depending on the total volume in the tank. A value with magnitude close to 1 indicate a strong relationship.

### 3. Implementation

---

Since the correlation analysis in Section 3.1.1 with regards to angular orientations indicated a linear relationship, a linear model is fitted to the data for each measurement series. Each measurement series has a different total volume and will result in a different linear fittings. Roll variation for a total volume of 35 litres is shown in Figure 3.2. A linear function is illustrated in the same figure, with the form  $\Delta V = A\Delta\theta_{Roll} + C$ .

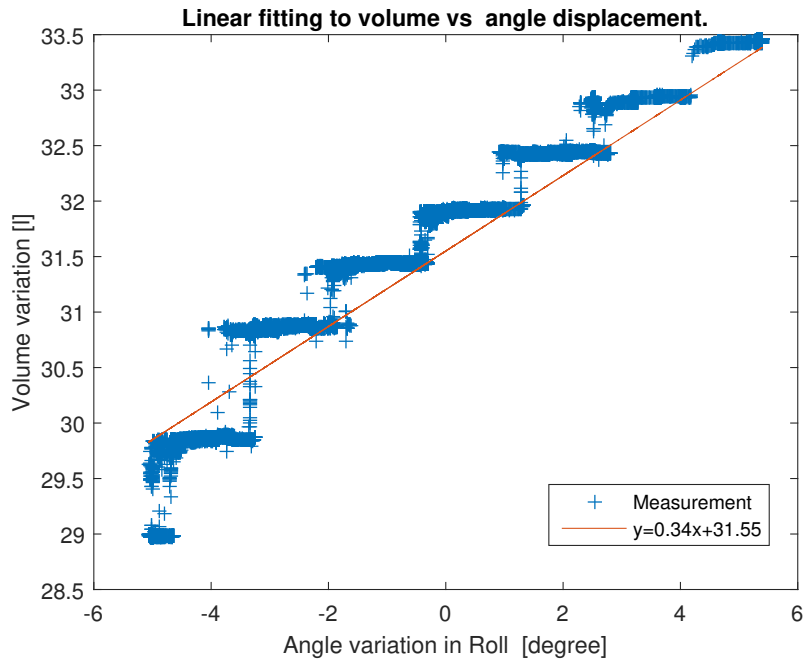


**Figure 3.2:** How the read values of volume change as the roll angle is varied. The measurements are plotted with a blue cross. A linear fitting is shown as a solid red line.

The magnitude of the fluid displacement changes as the total volume changes. Coefficients in the linear fitting will therefore also change. Figure 3.3 shows how coefficients A and C change depending on total volume. A high magnitude of A indicate a big change in volume reading as the angle vary.

### 3. Implementation

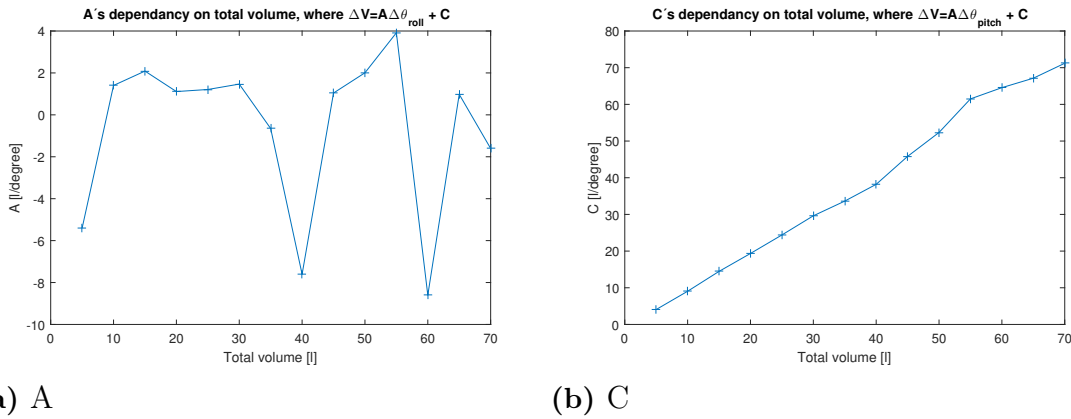


**Figure 3.3:** Coefficients  $A(V)$  and  $C(V)$  in the linear fitting  $\Delta V = A(V)\Delta\theta_{Roll} + C(V)$  are functions of the total volume,  $V$ . This figure shows the two coefficients the total volume vary from 5 litres to a full tank of 71 litre. The roll angle is varied.

Coefficients for the linear fitting as pitch is changed is showed in Figure 3.4.  $A$  has a large value for small total volume values, and is therefore large for the volumes close to 35 litre since the passive side starts to fill.

The active and passive sections of the tank is one reason for why the coefficients depend on the volume. The passive and active fuel level sensors are placed mirrored to each other. They therefore behave differently to angular displacements.

Which fuel sensor that has the largest effect on the readings depend on the volume. The angle error will have a small effect as long as the active side is full. The active side will have a large effect when the passive side is empty and the active side starts having a decreasing volume.

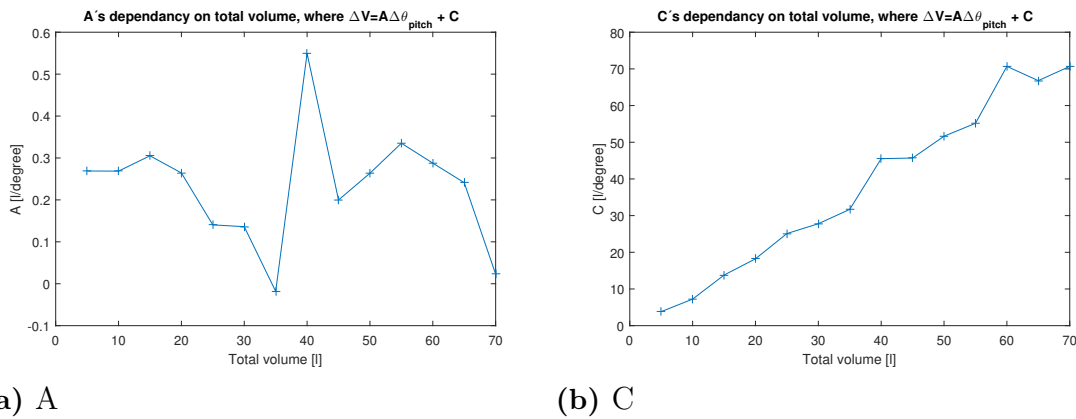


**Figure 3.4:** Coefficients  $A(V)$  and  $C(V)$  to the linear model fitted  $\Delta V = A(V)\Delta\theta_{Pitch} + C(V)$ . They change as a function of the total volume,  $V$ . The coefficients are shown as the total volume vary from 5 litre to a full tank of 71 litre. The pitch angle is varied.

A piecewise linear model is proposed since the parameters vary depending on the total volume in the tank. The angle parameters then change depending on the

current volume estimate. This means that the model will be non-linear, since the parameter depends on a state. Parameters for 14 different volumes are showed in Figure 3.3 and 3.4. A simplified model containing 4 parameters is made to avoid instabilities due to rapid changes in dynamics and to limit memory demands.

The values for 5, 20, 35 and 50 litres are saved, since they capture the behaviour of the almost empty and full tanks. Parameters are interpolated between the four given parameters as the volume estimate has changed more than one litre.

Acceleration and retardation of the vehicle will cause a change in fluid displacement in the tank. This is supported by Newton's second law. Acceleration in longitude and latitude could therefore be used in the measurement model. This would help with reducing misleading sensor results. Including acceleration in the measurement model can make the estimation of fuel level based on measurement easier. Unfortunately, it is difficult to perform an experiment that isolates the accelerations effect. A measurement model for acceleration will therefore not be presented in this report.

### 3.1.4 Final state space model

The different models derived can now be combined to create complete state space models. Two different state space models are used. They are referred to as the complex model and the simple model. The complex model include angle data, while the simple model is a simple integrator using only the consumption signal.

#### 3.1.4.1 Complex model

A measurement model can be constructed using the angle orientation model derived. The fuel level reading can be seen as the true volume plus the volume deviations described in the previous sections.

$$y = x_{lvl(k)} + p_{roll}(k) \cdot \theta_{Roll}(k) + p_{pitch}(k) \cdot \theta_{Pitch}(k) \quad (3.3)$$

where  $x_{lvl}$  is the true volume estimate value,  $p_{roll}$  and  $p_{pitch}$  are coefficients and  $y$  is the reading from the tank. The coefficients  $p_{roll}$  and  $p_{pitch}$  originate from the coefficients derived in the previous section. They have then been modified to better fit the purpose of making fuel level measurements less misleading while positioned in a slope.

This means that it is now possible to write the system in a state space form. The state space vector used, seen in Equation 3.4, includes the estimated volume and the angles roll and pitch.

$$\vec{x} = [x_{lvl} \quad \theta_{roll} \quad \theta_{pitch}]^T, \quad \vec{x}(k+1) = A\vec{x}(k) + B\vec{u}(k) \quad (3.4)$$

As described in Section 3.1.2, the next value of the volume can be described as the previous one minus the consumed fuel. This is described by the first row in the A and B matrix in Equation 3.5.

$$A = \begin{bmatrix} 1 & 0 & 0 \\ 0 & 1 & 0 \\ 0 & 0 & 1 \end{bmatrix} \quad B = \begin{bmatrix} -1 \\ 0 \\ 0 \end{bmatrix} \quad (3.5)$$

The time update relates the measurements to the states and uses the measurement model. Equation 3.3 is rewritten into matrix form as the first row in C:

$$C = \begin{bmatrix} 1 & p_{roll} & p_{pitch} \\ 0 & 1 & 0 \\ 0 & 0 & 1 \end{bmatrix} \quad \vec{y}(k) = C\vec{x}(k) \quad (3.6)$$

Note that there exist many different C-matrices, since the angle parameters depend on the current volume estimate. This makes the measurement model non-linear. It is however a piecewise linear model. The parameters are changed every one litre, making the change in parameter value small.

The remaining states, containing angle data, use a simple measurement model. The angle states are present to help get a more precise value of the fuel level. They are used as states to avoid having inputs in the measurement model. Having inputs in the measurement model makes it more difficult to design algorithms like the Kalman and  $\mathcal{H}_\infty$  filters. Using them as states instead of inputs can however have the same effect. Increasing the weight on the measurement model and having a small weight on the state transition makes the estimate behave close to an input.

#### 3.1.4.2 Simple model

This section describes an alternative state space model. It has the same state transition matrix, shown in Equation 3.5, but with only the fuel level as a state. Instead of having angles in the measurement model, it simply assumes that the volume measurement is equal to the volume state plus Gaussian distributed noise. This is expressed as a state space model, seen in Equation 3.7 and 3.8.

$$x = x_{lvl}, \quad x(k+1) = 1 \cdot x(k) - 1 \cdot u(k) \quad (3.7)$$

$$C = 1, \quad y(k) = Cx(k) \quad (3.8)$$

The simple model is used to evaluate different filter structures further on in the report. It is simpler to integrate than the complex model. Due to the simple nature of the model it was preferred to compare different filter structures with this model.

### 3.1.5 Properties of the state space models

A complete state space model is now developed. In this section the properties of the state space are evaluated.

A discrete state space system is asymptotically stable if and only if all eigenvalues of the A matrix are within the unity circle. The eigenvalues of the A matrix in Equation 3.5 are on the edge of the unity circle. This means that the system is marginally stable. The state transition matrix, A, can be multiplied with a value somewhat less than 1 to ensure asymptotic stability. [24]

A system is completely observable if there always is a time  $t_0$ ,  $t_0 < t_1$ , for which the state can be uniquely determined given measurement up to time  $t_1$ . A

n-dimensional linear time invariant system is completely observable if and only if the observability matrix, seen in Equation 3.9, has full rank. [25]

$$\mathcal{O} = [C \quad CA \quad \dots \quad CA^{n-1}]^T \quad (3.9)$$

The observability matrix for the matrices presented in the previous section has rank 3 for the complex model, for all combinations of angle parameters tested. The rank is 1 for the simple model. It implies complete observability for both models. This is a desirable property, since it otherwise would not be possible to implement successfully in a Kalman filter. [26]

## 3.2 Recursive Least Squares

This section presents an alternative parametric model in regard to the simple and complex state space models. It only needs lateral and longitudinal acceleration as well as raw fuel level readings to estimate the fuel level.

### 3.2.1 Fuel displacement due to acceleration

It is hypothesised that lateral acceleration and longitudinal acceleration will cause the liquid in the tank to move and therefore are disturbance factors. This claim is supported by Newtons second law.

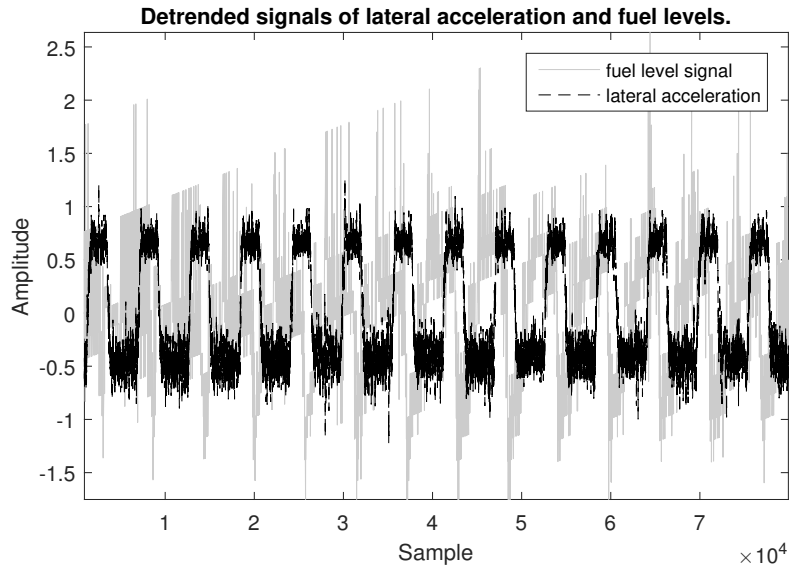


**Figure 3.5:** Two detrended signals, fuel level measurements and lateral acceleration. The correlation coefficient between the signals is -0.2138. The continuous line is the measured fuel level whilst the dashed line is measured lateral acceleration

The data presented in Figure 3.5 is given by VCC and shows fuel level readings of a fuel tank whilst the car is driving with extreme lateral acceleration. The car is driving in an eight-shaped test track. It is aesthetically visible that acceleration

and fuel level signals behave similarly. As the acceleration is increased the measured fuel level is decreased. As mentioned in Figure 3.5 there is a negative correlation at around 21 percent which indicates a strong linear relationship. The data showed in this section originate from extreme acceleration, making the trends easier to locate. The data sets have also been detrended, meaning that the declining trend of the fuel level is not present. This makes the similarities between the acceleration and level measurements larger.

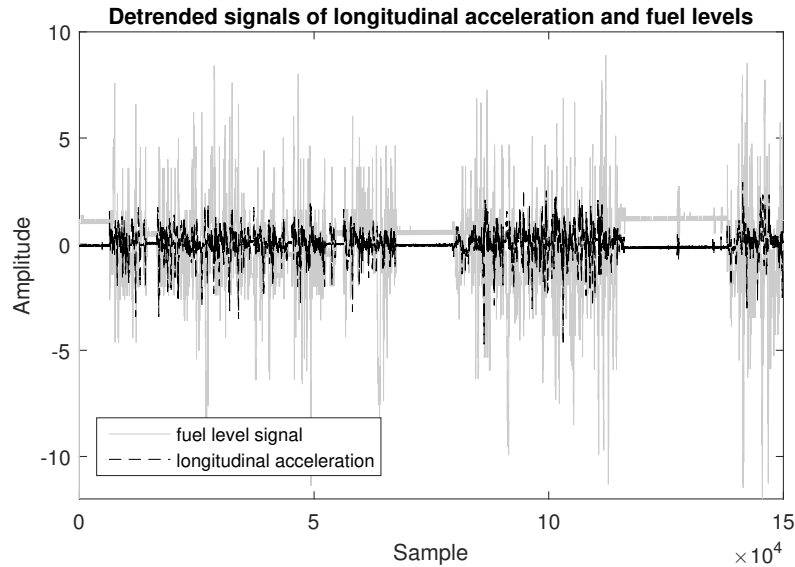


**Figure 3.6:** The graph shows two detrended signals. The correlation coefficient between the signals is -0.3280.

The measured fuel level and longitudinal acceleration for a data set where the car has heavy longitudinal acceleration can be seen in Figure 3.6 and is linearly related with a correlation coefficient of -32.8 percent. This relationship is reasonable, as the car stops and starts the liquid will have to move with the car. If there are heavy accelerations involved then the body of liquid should slosh. [4]

The acceleration of the car is measured by accelerometers. Since the gravity affects the accelerometer can the acceleration signals be used to capture the angle orientation of the car. By using the acceleration signals in the model, instead of the angle signals, can both the driving pattern and the car orientation be included in the model.

### 3.2.2 RLS model formulation

Through the experiment described in Section 2.5, it has been shown that there is a clear relationship between biased fuel level and angular orientations. However this relationship is non-linear and therefore a linear model would not suffice under various tank volume conditions. It has previously been described how a piece wise linear model relating angle to fuel displacement was created in Section 3. This section describes another approach. Instead of switching between a fix set of parameters, a

dynamic model is proposed. Therefore a model structure that fits the RLS algorithm will be investigated.

The method in which a model is made is through the grey-box modelling concept. It is known that the liquid in the tank and its sloshing phenomena is affected by acceleration. However how exactly the acceleration influences liquid dynamics in the fuel tank, the structure of the model and its order, is unknown.

Through experimental results and with regards to the results shown in this section, it seems clear that acceleration influences the sloshing mechanics in a linear way. However as discussed earlier this relationship is evolving as a function of acceleration and volume of liquid in the tank.

The modelling structure used will be of a ARX type model. This model is shown in the equation below:

$$y(k) = \theta_{lat}a_{lat}(k-1) + \theta_{lgt}a_{lgt}(k-1) + \theta_{lvl} \quad (3.10)$$

Where  $a_{lat}$ ,  $a_{long}$  are lateral and longitudinal acceleration signals,  $\theta$  is coefficients and  $y(k)$  the measured fuel level signal. Equation 3.10 shows the equation that will be used in the RLS algorithm. The coefficient  $\theta_{lvl}$  models the estimated fuel level. The product of the acceleration,  $a_{lgt}$  and  $a_{lat}$ , and the corresponding coefficients,  $\theta_{lgt}$  and  $\theta_{lat}$ , model the fuel displacement that occur due to acceleration of the car.

Therefore the online minimisation problem is:

$$\min_{\theta_{lat}, \theta_{lgt}, \theta_{lvl} \in \Theta} \sum_{k=1}^m (y(k) - (\theta_{lat}a_{lat}(k-1) + \theta_{lgt}a_{lgt}(k-1) + \theta_{lvl}))^2 \quad (3.11)$$

where  $m$  is the horizon. For each iteration in this weighted least squares minimisation problem the variable  $\theta_{lvl}$  is the estimated fuel level.

### 3.2.3 Robustness

This method is robust to different fuel tanks and varying dynamics. It minimises the cost function online, and therefore finds coefficients that model the fluid behaviour in the closest history. This makes it robust to different tanks and ageing tanks, in contrast to the static state space models described earlier in this chapter.

## 3.3 Filters

The Kalman,  $\mathcal{H}_\infty$  and particle filters are presented in this section. This section also describes the implementation of the models described in section 3.1.4 into these filter structures described. The objective is to compare the different filter structures that obtains the most robust volume estimation.

Only the Kalman filter was implemented using both the models. The Kalman,  $\mathcal{H}_\infty$  and particle filter were implemented using the simple model, with no information using angles. This was done as it was more time consuming to implement the complex model and it was therefore not possible to implement both models for all of

the filter structures. The simple model was therefore used to compare the different filter structures. The models share the same state transition model, which is heavily trusted compared to the measurement models in all filter structures. It was assumed that if one filter structure was proven better than the other with the simple model, it would also succeed better with the complex one.

The five filter structures investigated are therefore:

- Kalman with simple model.
- Kalman with complex model.
- $\mathcal{H}_\infty$  with simple model.
- Particle filter with simple model.
- RLS, described in Section 3.2.

#### 3.3.1 Steady state Kalman and complimentary filter

The steady-state Kalman filter and complimentary filters were considered to be of interest. These filters both used the simple model as described before. However they will not be included in the comparison, since their behaviour were very similar to recursive Kalman filter with the simple model.

The complimentary filter was considered more difficult when it came to implementing models with angles and acceleration, since it does not use measurement models in the same clear way as the Kalman filter does. It also showed similar behaviour as Kalman filter, but did not have any other advantages. Therefore the filter as mentioned was disregarded.

The steady state Kalman filter also behaved similar to recursive Kalman filter. One drawback of the steady state Kalman filter is that it is more difficult to implement nonlinear models. Therefore the steady state version was disregarded as the complex model is non-linear.

## 3.4 Comparison of filter structures

This section will compare and present five different types of model combinations and filter structures. The objective of this comparison is to conclude which filtering method provides a robust estimation and from there further develop these filtering methods. Things that will be tested are the convergence time, response time of online and offline refuelling, estimation of fuel levels in inclined parking situations and lastly their computational demands.

#### 3.4.1 Convergence

The previous estimated value of the fuel level is saved before the car is turned off. Once active again the previously saved value is used as a initial state. However under some circumstances the initial value could be incorrect. Such errors can arise under situations where fuel is used for heating or if fuel has been removed from the tank. It is therefore important that the filters will adapt to the new true volume at the same time with minimal noise or fluctuations. The time it takes for the filter to

converge to the new volume is called convergence time and is the number of samples multiplied by the sampling time.

**Table 3.2:** Time needed before filter has converged. Convergence time is showed in minutes.

Filter Initial offset [l]	-15	-10	-5	0	5	10	15
Kalman with simple	2.3	1.9	1.3	0	8.8	8.8	8.8
Kalman with complex	2.3	1.9	1.3	0	10.1	10.1	10.1
Particle filter	6.8	4.9	2.7	0	8.3	15.3	16
$\mathcal{H}_\infty$	0.2	0.1	0	0	0.3	0.3	0.3
RLS	0.1	0.1	0.1	0.1	0.1	0.1	0.1

Table 3.2 shows the convergence time in minutes, as the initial state value offset is varied. The filter is said to be converged when it is less than 1 litre away from the stable measured fuel levels.

The Kalman based filters convergence time depends on the ratio between the Q and R matrices. A large quota indicates fast convergence, since the measurement update is weighted higher than the model prediction. As a result of a large quota, the filter will trust the measurement values heavily and therefore prone to following the noise characteristics of the sensor measurement. The tuning of the filters therefore play a large roll in the convergence time. The filters have been tuned so that they behave smooth on legal city and highway driving.

The RLS based filter has the lowest overall convergence time, which is not surprising. RLS can be seen as a Kalman filter without the prediction step, which increases the dependency of the measurement values.

The particle filter has the longest convergence time for almost all initial offset values. This also depend on the quota between the R and Q matrix. It also depends on number of particles. 50 particles are used in this filter, which is a large number. Having a lower number resulted in noisy behaviour and insufficient estimates.

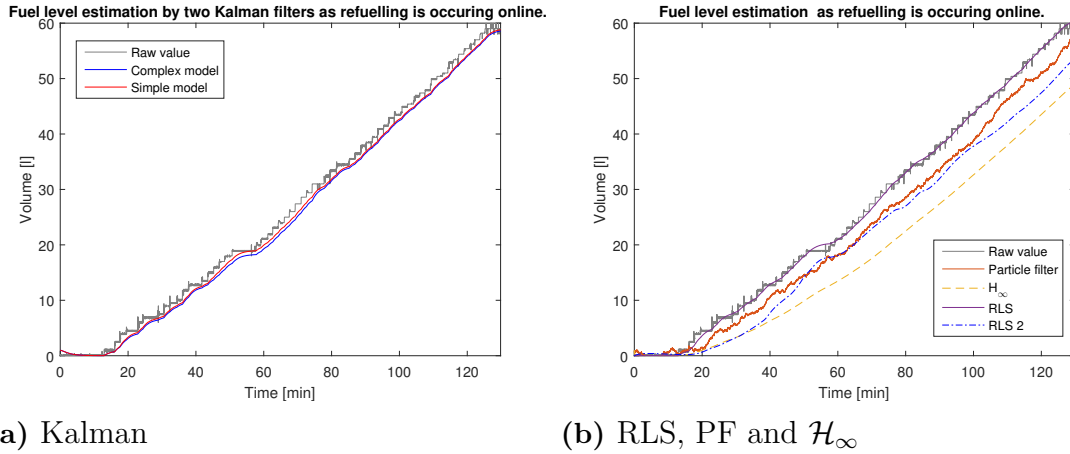
#### 3.4.2 Online refuel detection

If the vehicle is active, i.e. not turned off, while refuelling neither the simple nor the complex state space model will be correct. The state transition model in all models predicts that the consecutive value should be the previous one subtracted the consumed fuel. This is not true while refuelling. Refuelling often takes place offline, i.e. turned off. However, it may be necessary to keep the car on in cold conditions. It is also possible to keep the car on at manned refuelling stations, where the staff refuels the car.

Table 3.3 shows estimator quality indicators for the estimators compared to the raw value. The raw value is used since it has a relatively small co-variance while refuelling due to the steady position of the car. The estimates together with the raw value is shown in Figure 3.7.

**Table 3.3:** Mean square error, variance accounted for and covariance for the different filters compared to the raw signal as new fuel is inserted.

Filter	MSE	VAF	Correlation	STD
Kalman with the simple model	1.22	0.999	0.9996	0.59
Kalman with the complex model	2.03	0.9986	0.9994	0.6892
Particle Filter	12.7	0.9915	0.9981	1.72
$\mathcal{H}_\infty$	74.36	0.9580	0.9949	3.8323
RLS	27.86	0.9859	0.9967	2.2186



(a) Kalman

(b) RLS, PF and  $\mathcal{H}_\infty$

**Figure 3.7:** Fuel level estimations as the tank is refuelled. Subfigure 3.7a shows Kalman filter based on the simple model, the complex model as well as the steady state Kalman. Subfigure 3.7b shows the particle filter,  $\mathcal{H}_\infty$  and the RLS filter.

All filters behave in a sufficient way as the tank is refuelled. This may be as a result of the slow paced nature of the refuelling in this data set. This gives enough time for the filters to converge to the increased fuel levels.

### 3.4.3 Detect offline refuelling

Detecting whether refuelling has taken place as the vehicle was turned off can also be problematic. This is related to Section 3.4.1, where the convergence time for the filters were investigated. It is important that the level indication adapts quickly to refuelling, as it is confusing for the driver if an empty tank is indicated directly after refuelling. It is therefore important that a refuelling is detected quickly after the car is turned on after a refuelling.

Refuelling to a full tank offline will also lead to problems, since the floater has trouble giving a sufficient volume reading in that region. It can therefore be difficult to decide if the tank was refuelled to a full tank or somewhat less.

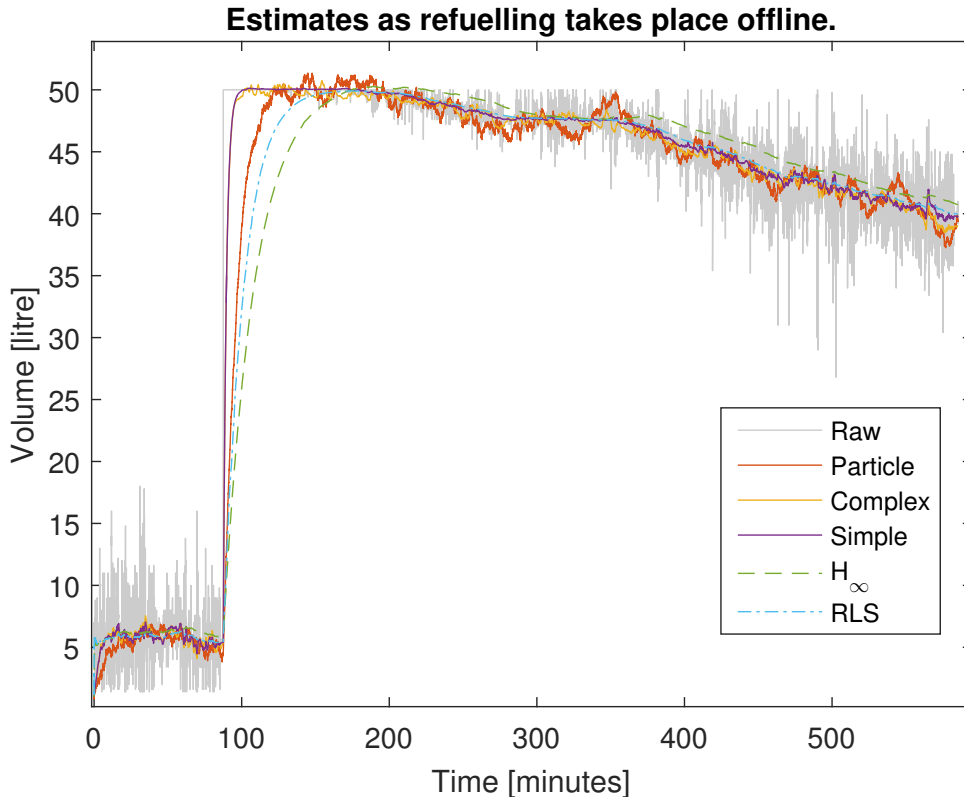


**Figure 3.8:** Fuel level estimate as the vehicle is turned off around, refuelled and then turned on.

Figure 3.8 shows the five estimator values as the vehicle is turned off, refuelled and then turned on. All five converge slowly towards a full tank. Both Kalman filters converge over approximately 10 minutes, whilst the particle filter converges over approximately 39 minutes.  $\mathcal{H}_\infty$  converges the slowest, which is due to tuning.

Both Kalman filters behave similar in both the online and the offline refuelling. This is expected, due to the horizontal placement of the car in a refuelling situation. The complex model based Kalman filter uses angle data in the measurement model, which the simple does not. Angular orientation is close to a constant value for these two data sets since the car is placed stationary on a horizontal surface. The simple and complex models behaves similar as angular orientation is kept close to zero.

### 3.4.4 Large angles

Parking or driving in a tilted position can be a part of the everyday driving routines for some drivers. It has been previously discussed and shown that different angular orientations will give a misleading fuel level reading due to a change in fluid displacement. It is therefore important that the filter predictions are not affected by such situations. Angular orientations under long periods lead to many misleading fuel level readings, which can lead to the assumption that either refuelling or removal of fuel has occurred which is simply not the case.

To test the filter’s performances under these conditions, several experimental driving cycles were performed and the corresponding data was collected. The car

was filled up with three different volumes of fuel: 5, 20 and 50 litres.

The volumes were chosen in such a way to test the different positions of the floater arm: the active arm close to the bottom, the active arm in the middle and the passive arm in the middle.

Six different positions were tested for each volume. The first four were: car frontal upwards, car frontal downwards, driver side downwards, driver side upwards. Two combinations of the basic positions were then tested to see if the assumption of superposition was correct. Car frontal upwards while driver downwards and car frontal downwards while driver downwards were therefore tested. The pitch was tested as the car frontal was upwards or downwards. The roll angle was tested when the drivers side was up or down. How the filters handled three of the positions for one of the volumes will be showed in this section. The reasons for not showing all 18 data sets is due to the filters behaving similar on all of them.

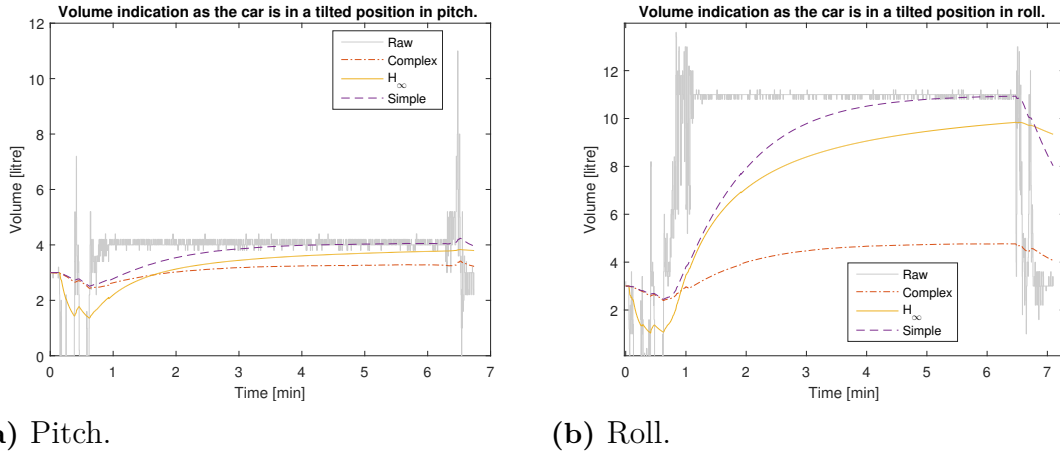
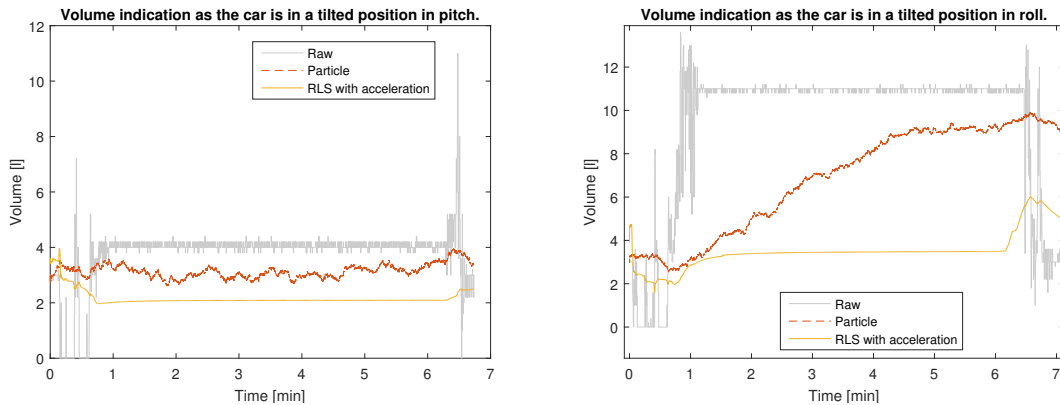


**Figure 3.9:** The raw volume readings together with Kalman and  $\mathcal{H}_\infty$  estimates as the car is driven into a tilted position. The car stands in the tilted position for approximately 5 minutes before driven down to flat surface.

Figure 3.9 shows the fuel level readings along with the Kalman based estimations as the car is positioned in a hill. The inclination varies in the hill, but the car is positioned in a spot where it is measured 14.5 degrees. The sequence start as the car is standing still at the end of the hill in a horizontal position. The fuel level reading in this position indicate a value close to 3 litres. The car then drives up the hill, resulting in large variance in raw value. In the following 5 minutes the car is standing still in the hill. Subfigure 3.9a has the cars frontal side pointing downwards and subfigure 3.9b has the driver side of the car pointing downwards. The raw fuel level readings indicates a larger volume as the car is standing still in the hill. At the end of both sequences the car is driven down to the horizontal position at the end of the hill.

The simple Kalman filter and the  $\mathcal{H}_\infty$  filter which does not include angle data in the models start to converge to the larger volume data. The Kalman filter which do include the angle data, referred to as the Complex one, does not adapt in the same extent. This is a desired behaviour, and point to the necessity of using the angle data.

### 3. Implementation

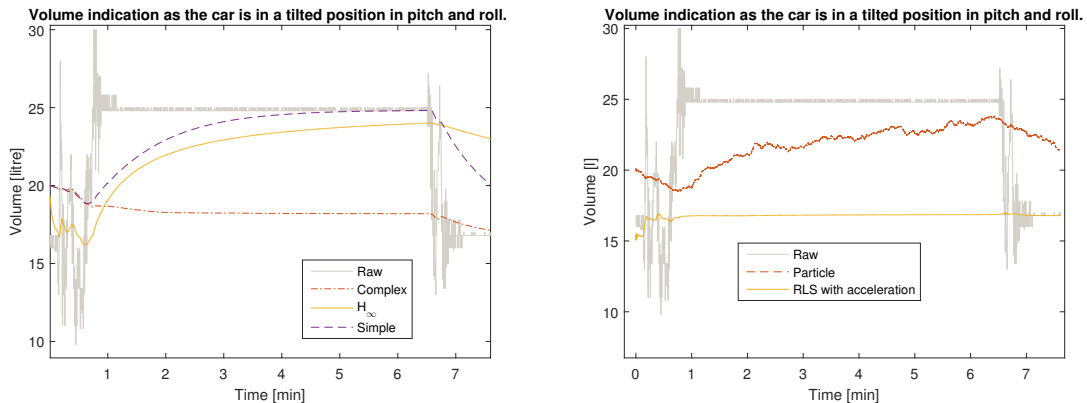


(a) Pitch.

(b) Roll.

**Figure 3.10:** The raw volume readings together with RLS and PF estimates as the car is driven into a tilted position. The car stands in the tilted position in approximately 5 minutes before driven down to flat surface.

Figure 3.10 shows the same data sets as 3.9 as the RLS algorithms together with the particle filter are applied. The RLS with acceleration data keeps the true indicated volume even in the tilted position, which the particle filter does not.



(a) Kalman and  $\mathcal{H}_\infty$

(b) RLS and PF

**Figure 3.11:** The raw volume readings together with Kalman and  $\mathcal{H}_\infty$  in a and RLS and PF estimates in b as the car is driven into a tilted position. The car stands in the tilted position in both roll and pitch and is in the position for approximately 5 minutes before driven down to flat surface.

Figure 3.11 shows the different estimators estimate the level as the car is in a tilted position in both roll and pitch at the same time. The hypothesis of superposition between the two angles seem to be acceptable, as the complex model based Kalman filter behaves sufficient.

#### 3.4.5 Computational power

Each and every algorithm that is mentioned computes an estimate with different amounts of CPU operations. This section will describe the computational complex-

ity of the algorithms within the thesis.

The scope of this evaluation is to evaluate the running time and memory usage of the algorithms in a online manner. This concerns only the running time for a single iteration as all algorithms will be run online.

### 3.4.5.1 Running time

The values within Table 3.4 were brought out through running all these algorithms under one iteration 1842452 times and taking the mean of the running times. These algorithms were tested on a Intel i-7 6600U CPU vPro edition

**Table 3.4:** Running time of various filter algorithms under one iteration

Filter	Time (s)
Steady state Kalman	$3.8664 \cdot 10^{-7}$
Recursive Kalman	$7.9006 \cdot 10^{-4}$
RLS using acceleration	$2.4043 \cdot 10^{-5}$
Particle Filter	$1.6 \cdot 10^{-3}$
$\mathcal{H}_\infty$	$1.7702 \cdot 10^{-4}$

It is visible from Table 3.4 that most of the filter run quickly. All run well under one second for a single iteration. However to conclude they would work efficiently in a ECU is still a question to be answered. Therefore further investigations are required. The computational steps for each and all the algorithms are minimal, however the only algorithm that could be of concern is the particle filter as its complexity grows with an increase in particles. The steady state Kalman filter is included to show how fast the filter runs once it has converged.

### 3.4.6 Conclusion of filter structure comparison

All of the five filters investigated showed good performance, most behaved similar on the majority of qualities tested. Only the complex Kalman filter and the RLS behaved desirable under angular conditions, which was expected as the others did not use angle data. Since no filter is exactly perfect the two most desired filter structures were chosen based on simplicity and predictive performance. These filters are chosen and further developed on. The two filters that were chosen were further tuned, some extra functions were implemented and were tested as well.

The majority of the filters behaved similar on the online refuelling case and have similar complexity and memory demands. The offline refuelling case also resulted in similar result. It is therefore difficult to draw a conclusion. The tilted position test however, resulted in large variations in result. The Kalman filter and the RLS algorithm with angle and acceleration data respectively gave a truer indication compared to the other filters. The PF was disregarded as it did not provide a smooth estimate as the Kalman and  $\mathcal{H}_\infty$  did. It is also worth noting that the  $\mathcal{H}_\infty$  filter was disregarded as it has more variables to tune than the Kalman filter with performance similar to it. Therefore to keep things simple it is better to choose a more widely used and easily tune-able filter.

## 3.5 Final Filters

The two filter structures that were chosen to be proceeded were the Kalman and RLS filters and both needed further development. Both filters would benefit from the ability to detect whether refuelling is or has occurred. This would make it possible to have a slow responding filter under normal driving conditions as it could be assumed that a increase in fuel volume will not be happening.

When refuelling is detected the filters can be tuned to respond quicker to such quick fuel level increases.

### 3.5.1 Online refuelling detection

In some VCC cars, for example the XC60, the tank lid is opened by an electronic signal. [27] It is logical to use this signal in the detection of online refuelling. As long as the lid of the fuel tank is closed then no fuel can be added into the tank.

A state can be constructed where the state requires a open lid and zero velocity signal. Once this state is true the filters can be re-tuned to respond quicker. The Kalman filter is tuned in such a way that it trust the measurement more or trusts the model less when the state is true. The RLS re-tunes the lambda value which lowers the trust on previous measurements as the lid is opened.

### 3.5.2 Offline refuelling detection

The state of the lid signal cannot be detected once the car is turned off and all car models produced can not detect the opening of the tank lid. Therefore the filters cannot always detect whether refuelling has taken place. It is therefore necessary to detect whether refuelling has occurred every time the car is turned back on.

An offline-refuelling state is introduced, which is true if offline refuelling is detected. Refuelling can be seen as a step response and therefore it is important to look at the impulse response of the fuel level signal. This is done by taking the difference between the last volume estimate and the new volume measurements, after the new measurements have been angle corrected. There should be a significant difference if the driver has refuelled. The angle model described in Section 2.5 is used both for the Kalman and the RLS filters.

If offline refuelling is detected, the filter enters a similar state to online refuel detection. The filters heavily trusts new measurements rather than model based predictions.

### 3.5.3 Low fuel levels

The floater arm is not capable of providing reliable information past small volume readings. This has been discussed previously and relates back to physical limitations of the floater arm. The estimation of the consumed fuel is however independent of the volume in the tank. When the filters detect a low fuel level and does not detect online refuelling, it is therefore reasonable to trust the consumption signal completely.

From there on the filters use dead-reckoning with the use of instantaneous fuel consumption to predict the fuel levels.

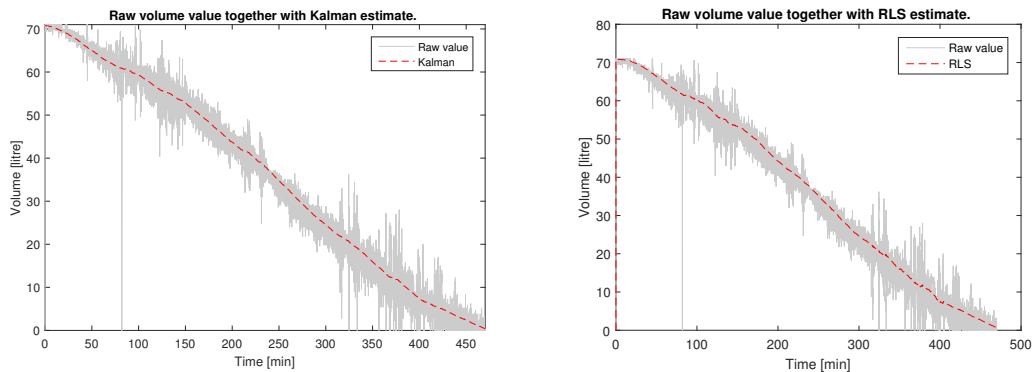
The fuel consumption signal has an approximate uncertainty of  $X\%$ . This uncertainty could be added as additive parametric uncertainty to the B matrix in the Kalman filter when the volume estimate is smaller than a fixed small fuel volume. This in theory should make it more robust. The uncertainty was increased to  $Y\%$ , with  $X < Y$ , to avoid estimating more fuel than the true value due to entering the dead reckoning mode at a too low fuel volume.

### 3.6 Filter evaluation

To look at how robust filters are it is important to test the filters with data sets that were not used in the tuning and the designing of the filters. This method will show how robust the filters are outside of data sets used to tune it. Therefore if the filters are able to perform well under many different types of unknown conditions, the filters could be considered robust.

The two filters that were proceeded with are evaluated using seven sets of previously unused data. The data sets are collected from real driving scenarios in various cars and therefore belong to different kinds of tanks. Data is presented along with the Kalman and RLS estimate. The estimates are evaluated based on what is assumed reasonable. It is important to point out that the true volume value is unknown with the exception to when the tank is completely empty.

Throughout this section, the raw fuel level values are shown in light grey and the estimates are shown as a crosshatched red line.



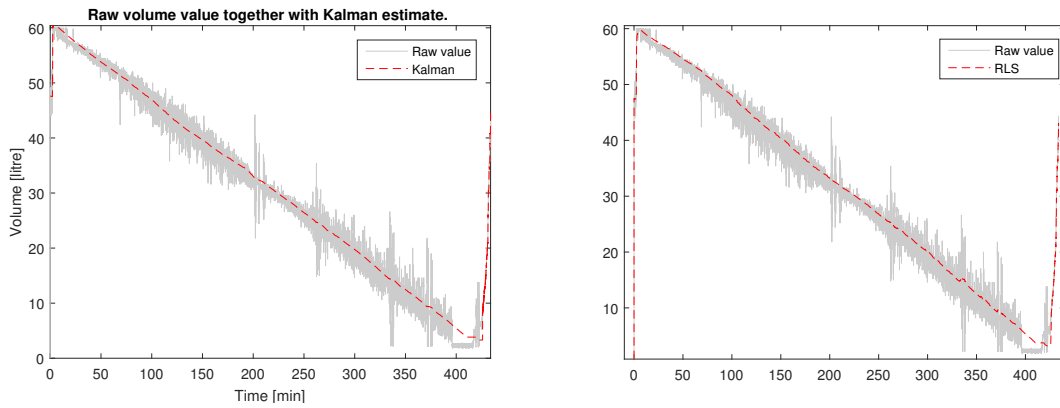
(a) Kalman estimator.

(b) RLS estimator.

**Figure 3.12:** Kalman and RLS estimates based on a drive from a full to an empty tank. Both estimators give a stable value throughout the drive. Kalman estimator have a value closer to zero as the car stops.

Figure 3.12 shows the Kalman and RLS estimate for a driving cycle using a 71 litre tank. The driving cycle is from full tank to engine stop due to no available fuel. The driving pattern differs through out the cycle, making the variance of the raw measurement vary.

### 3. Implementation

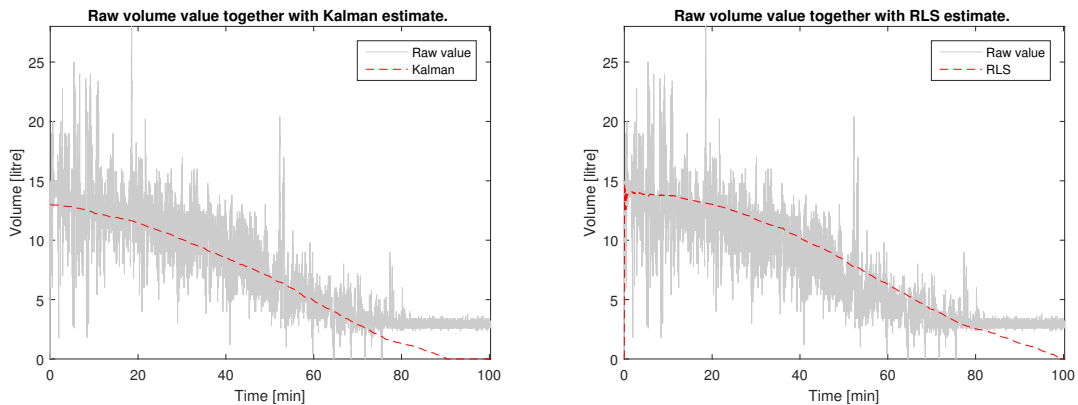


(a) Kalman estimator.

(b) RLS estimator.

**Figure 3.13:** Raw values for a drive cycle from full tank to engine stall. The cycle ends with an online refuel. Both Kalman and RLS estimate the empty tank closely before the engine stalls.

A drive cycle from a full 60 litre tank to engine stall is shown in Figure 3.13. The tank is refuelled at the end of the driving cycle in the online mode. RLS indicates a volume value of 3.7 litres at engine stall. One patch of data is missing, making the raw values drop directly from 6 litres to 2 litres. Therefore both Kalman and RLS indicate a nonzero value at engine stall. This shows how much both filters rely on detecting online and offline refuelling or hosing. However, in this case this is not a weakness of the filters but rather that the data set is missing information. After the engine stalls, the tank lid is opened and both filters enters the online refuelling mode.



(a) Kalman estimation.

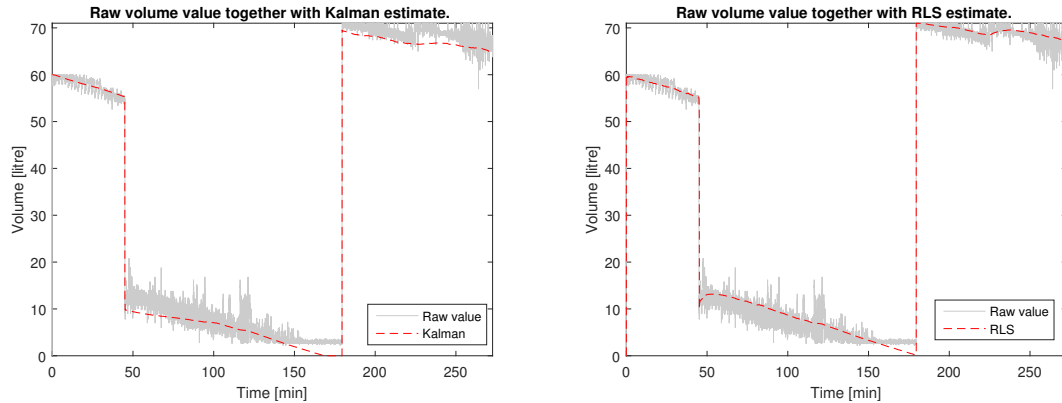
(b) RLS estimation.

**Figure 3.14:** Raw volume measurements as a car is driven to engine stop due to missing fuel. Both the Kalman and the RLS estimation estimate zero volume before the stall.

Figure 3.14 shows a cycle from approximately 15 litres to empty. The initial value means that the active side was close to half full as the tank had a total volume of 71 litres. Both the Kalman and the RLS provide a smooth estimate and indicate

### 3. Implementation

a zero value at the end. The curvature of the estimate differs between the filters. This can be derived from the Kalman filter's large dependency on the consumption and the RLS dependency of the raw volume value. The Kalman estimation indicates zero volume approximately 7 minutes before the final stop due to lack of fuel and the RLS circa 1 minute before. It is also worth noting that the Kalman filter on start up is more stable than that of the RLS filter. If the co-variance matrix is set to zero on start-up then the RLS predictions will fluctuate until the covariance matrix stabilises.

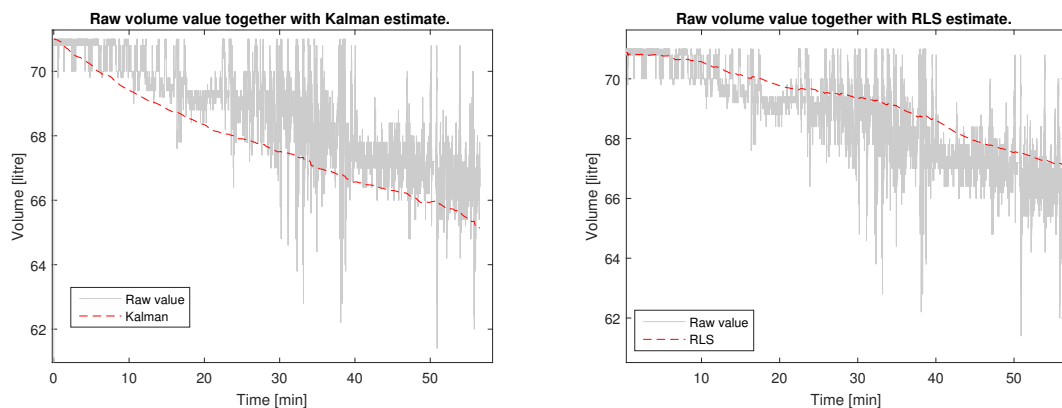


(a) Kalman estimation.

(b) RLS estimation.

**Figure 3.15:** A driving cycle including hosing, driving to empty, refuelling to full tank and finally normal driving. The Kalman and the RLS both indicate zero before the engine stop, with Kalman estimating an empty tank first.

The driving cycle presented in Figure 3.15 starts at approximately 60 litre. The car is then turned off and approximately 45 litres were extracted. The car is then turned on once again, and driven to an empty tank. Both estimators indicate zero volume at engine stall. The Kalman filter indicates an empty tank 3 minute before the RLS. The car was then refuelled to a full tank, approximately 71 litres.



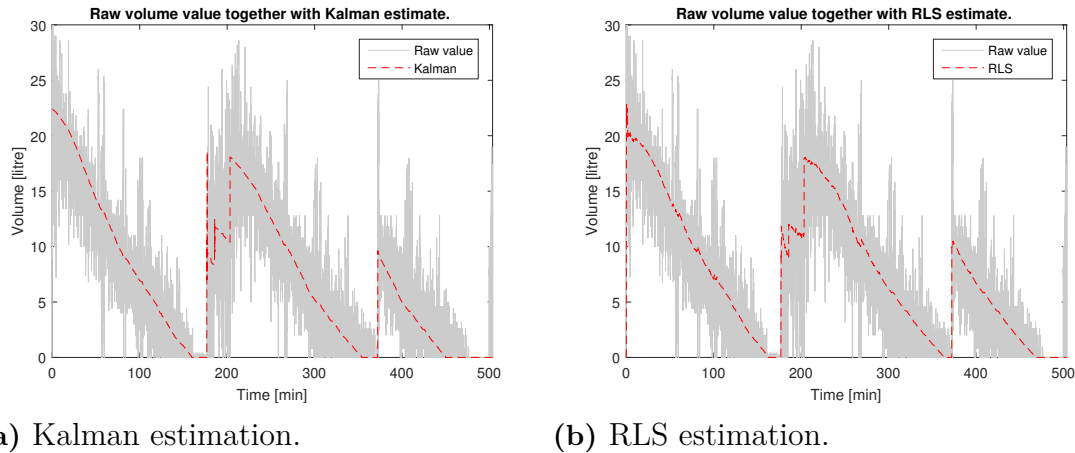
(a) Kalman estimation.

(b) RLS estimation.

**Figure 3.16:** Driving from a full 71 litre tank. The Kalman filter and the RLS filter estimate different fuel levels, with Kalman estimating a lower volume.

### 3. Implementation

Figure 3.16 shows a driving cycle from a 71 litre tank. It shows driving from full tank. Note that Kalman and RLS indicate approximately 65.6 litre and 67.1 litre respectively at the final instance. The big difference could originate from the Kalman depending on the consumed fuel and RLS on the raw volume measurements. Since the floater arm is not giving sufficient readings at the top position, the measurements can be misleading. It is not possible to conclude what estimate is closer to reality since no true value is given.



(a) Kalman estimation.

(b) RLS estimation.

**Figure 3.17:** Driving from circa one third full tank to empty twice, followed by one sixth full to empty. The first refuelling is done in steps. The Kalman estimate zero remaining fuel before the RLS does for both engine stops.

Figure 3.17 shows a driving cycle for a car with a 60 litre tank. The car start with approximately 24 litres and drives to empty. It is then refuelled in 3 rounds, until it reaches approximately 20 litres. It is then driven to empty once again and refuelled. Lastly it is driven to empty once again. The Kalman estimation shown in Figure 3.17a, indicates zero volume shortly before all engine stalls. The same applies for the RLS filter, seen in 3.17b.

The overall impression after looking at these driving cycles is that both estimators behave in a smooth and stable manner. The online and offline refuelling detection seem to work, but both filters behave noisier as they detect the online refuelling. Kalman and RLS both reach zero indication before the engine stalls, with Kalman reaching it some minutes before. This is a tuning property, and can be changed. What is preferred, reaching it long before or as precise as possible, can differ. It is important however, that all filters reach zero before the tank is empty.

# 4

## Discussion

This chapter discusses different aspects on the project. The results and the uncertainties are discussed, followed by suggested future work.

### 4.1 Filter evaluation

This section discusses and evaluates the two final filters, the Kalman and RLS filters, based on the result in Section 3.6.

#### 4.1.1 Evaluation uncertainties

As previously mentioned, it is inherently difficult to conclude whether any of the filters investigated give an accurate prediction. The only reference value available is when the car comes to a stop as a result of an empty fuel tank. This is visible through the velocity data. Conventionally the prediction performances of filters are assessed numerically with regards to some true value. However there are no actual reference values or true fuel level volumes to compare to. Because of such issue it is not possible to evaluate the filters performances properly in a numerical way, that is looking at the mean squared error, standard deviations etc. Therefore assessing can be done through qualitative methods, by looking at the visual properties of the filters. This assessment is done by looking at how the filter follows the noisy fuel level trends and how stable it is. However such assessment is subject to the designer of the filter and could be influenced by faulty intuition or bias.

#### 4.1.2 Filter behaviour

Both the Kalman and RLS filters indicate a fuel level close to zero before the car stops as a result of an empty tank. It is visible that the Kalman filter has a tendency to indicate zero faster than the RLS filter. What is preferred may differ and depend on requirements. Indicating zero fuel close to the engine halt will increase the indicated driving range. Such behaviour may be a desirable trait as it may be used as a selling point. However such traits may lead to over estimation which may lead to engine stalls during times where the car indicates a positive fuel level. The Kalman filter can be designed in such a way that it has a higher safety margin and for such engine halt situation to occur would be less likely.

Neither the Kalman or RLS filter are indicative of terrible predictions. None of the filters increase fuel level volumes unless refuelling is registered. However both

filters are largely dependant on the two following signals: fuel cap status and the state of the car, that is when it was off or on. If these signals were not present then the filter would not be able to detect refuelling with the proposed solution. Fuel lid state signal is currently available in the car network, however its function seem to be only available in some cars. However enabling the function of this signal for the next generation cars should be a relative simple and beneficial fix.

As discussed both filters are viable options for implementation, however visually it is possible to see that there are some differences between the filters. The Kalman filter is a more stable filter; the Kalman benefits from having two sources of information when it comes to fuel level predictions: the fuel level and the fuel consumption. The Kalman filter can easily be designed to converge to zero faster with adding additive parametric uncertainty to the B matrix.

The RLS type filter is more noisy than the Kalman filter, however tends to follow raw fuel level trends more than the Kalman filter. The filter is generally slower at converging to zero and by improving its converges rate one would have to re-tune the lambda value. Such tuning could possibly lead to a noisier estimates. However where the RLS performs well are situations where the car is parked in an angle. The RLS is able to change its dynamics to accommodate the non-linear dynamics of the system. Therefore it is effective in removing biased fuel level readings under angular orientations over different sets of fuel volume. In conclusion both filters are quite similar but as discussed has some advantages and disadvantages over each other. The most preferable filter would thereby have the best traits from both filters. These traits in the future could be combined into one filter for better future predictions of fuel levels.

## 4.2 Motivation of research methodology

Both filters are developed based on a 71 litre saddle based petrol tank. The tank and fuel type were chosen based on the preference that VCC had. It was also possible to use a real tank of this size and relevant data was available. Many different types of tanks were used during the evaluation. It is therefore difficult to point out faults that is either based on the data given or the filters themselves. The filters behaved as desired even without being specifically tuned for a certain tank type. There is a chance that the filters could yield a better prediction with some tuning.

## 4.3 Kalman frequency domain behaviour

Equation 4.1 shows the transfer function from the innovation,  $\bar{y} = y(k) - \hat{y}(k)$ , and the input consumption,  $q(k)$ , to the estimate of the measurement,  $\hat{y} = C\hat{x}(k|k-1)$ .

$$\hat{y}(k) = C \cdot (I \cdot z - A)^{-1} \cdot A \cdot K_k \cdot \bar{y}(k) + B \cdot (I \cdot z - A)^{-1} \cdot I \cdot z \cdot q(k) \quad (4.1)$$

where  $z$  is the shift operator. The function that the shift operator acts on is shifted one instance in to the future:  $z \cdot x(k) = x(k+1)$ . In this section the frequency characteristics of the transfer functions are investigated.

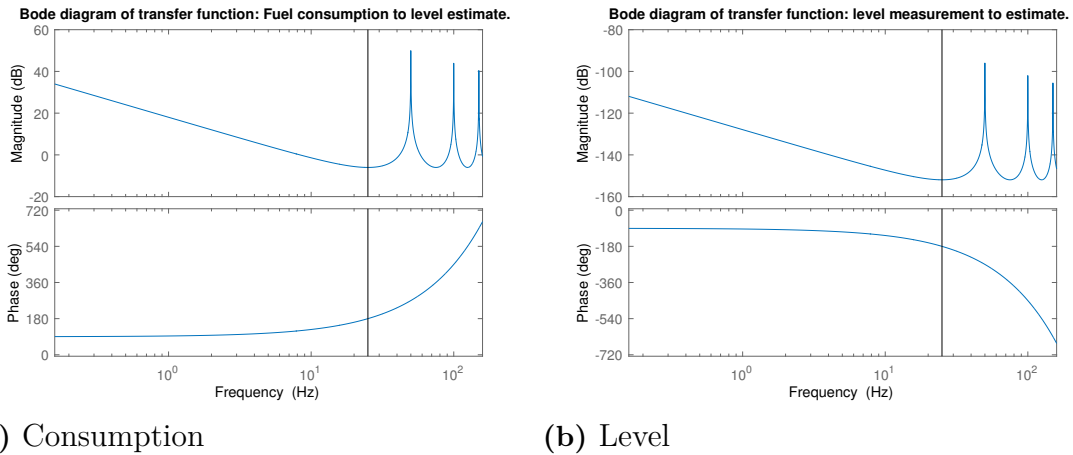


**Figure 4.1:** Bode plots for the transfer functions between the input fuel consumption and level estimate in a, fuel level measurement and estimate in b. The consumption to estimate act as an all pass filter, and the measurement to estimate act as a low pass filters.

It is visible from Figure 4.1 that the filter behaves similar to a lowpass-filter between the level measurement and the estimate. The attenuation is very high, making it close to an all-stop filter. This is more or less the case when the system dynamics are simple. The noise characteristics of the fuel level signal is in the high frequency spectrum. Therefore interesting information lies within the low frequency spectrum. However, the Kalman filter does not put a lot of faith in the measurement, making the attenuation high. The fuel consumption signal has its interesting properties within both the high and low frequency spectrum. The filter therefor behaves as an all-pass filter between consumption and estimate. Neither of the frequency responses behave sufficiently after 25 Hz. This is related to the sampling frequency being 50 Hz. Due to Nyquist and Shannons sampling theorem, which states that only frequencies up to half the sampling frequency can be reconstructed, this is expected. [28]

As a result from tuning the properties of the Kalman filter changes. It is therefore interesting to investigate the behaviour of the filter with different tuning. The quotient between R and Q,  $\rho = R/Q$ , determines the frequency response of the filter.

The singular values of the closed loop system will showcase the frequency response of the filter. The definition is shown in Equation 4.2.

$$\sigma(G) = \sqrt{\lambda(G^T G)} \quad (4.2)$$

The Kalman Frequency Domain Identity, Equation 4.3, offers an alternative way of describing the behaviour. [29]

$$(I + G_{KF}(j\omega))(I + G_{KF}(j\omega))^T = I + \frac{1}{\rho} C(j\omega \cdot I - A)^{-1} (j\omega \cdot I - A)^{-T} C^T \quad (4.3)$$

Where  $G_{KF}$  is the filter loop transfer function from innovation to the estimation.

The singular values for the Kalman gain can then be formalised as:

$$\sigma(I + G_{KF}(j\omega)) = \sqrt{1 + \frac{1}{\rho} \sigma^2(C(j\omega \cdot I - A)^{-1})} \quad (4.4)$$

The singular values depending on frequency is plotted in a log-plot and shown in Figure 4.2. The figure shows five curves with different tuning. The bandwidth of the filter changes as  $\rho$  is changed. The final tuning of the filter has  $\rho = 10^{10}$  and the figure includes  $\rho$ -values 10 and 100 times smaller and bigger. It can be concluded from the figure that a smaller  $\rho$  leads to a larger bandwidth. A smaller quota means a larger trust in the measurements and noisier estimate. Increasing the quota further would therefore limit the frequencies the Kalman can successfully map. However, the lower frequency spectrum is of most interest as change in fuel volume is a slow process.

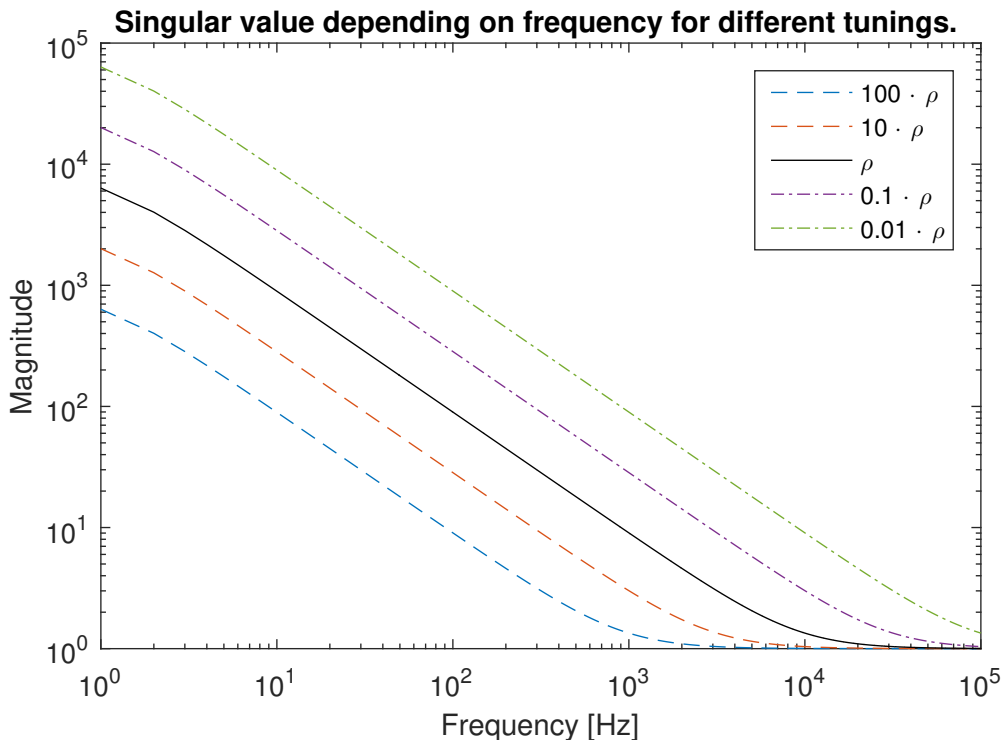


**Figure 4.2:** Singular value depending on frequency for different tunings. The tuning used in the final Kalman,  $\rho = 10^{10}$  is a solid black line. 10 and 100 times larger and smaller  $\rho$  is also shown.

## 4.4 Future Development

This section presents different suggestions and discussions on how this thesis could be continued and further developed on.

### 4.4.1 State detection

This thesis has mainly focused on the differences in prediction performances of various filter algorithms. However a problem that has been encountered in the thesis is the detection of nonlinearities. As discussed, these nonlinearities include offline and online refuelling. Online refuelling can be detected robustly with the use of the fuel lid signal. However offline refuel detection is more of a difficult problem. The system can detect refuelling only above three litres and at times can lead to noisy initial estimates. Therefore it would be beneficial to look at a robust method for offline fuel detection.

The noisy properties of the fuel level measurement change as acceleration changes. The relationship depend on the current volume. These nonlinear behaviours are difficult to quantify in a model. However it would be beneficial to investigate how to detect these nonlinear states robustly. Once these nonlinear states have been detected the filters can be re-tuned for the specific states in order to improve on the predictions of the filters.

### 4.4.2 The fuel consumption signal

The fuel consumption signal is directly related to how much fuel there is in the tank. This information is also crucial for the Kalman filter and its stable predictions. It has been observed that the fuel consumption signal is not fully accurate. Through future work it would be beneficial to investigate how to improve fuel consumption predictions. A method to do so is by looking at ways to model fuel consumption behaviour.

In order for good prediction it is worth improving the fuel consumption signal and therefore factors that influence and disturb fuel consumption. Velocity and acceleration are variables that influence such consumption and can potentially lead to models with 90 percent accuracy. Another factor includes road slope, a 1 percent inclination could increase consumption by 9 percent [30]. Power demands, engine RPM and heating within the car are also other factors [31]. Through intuition, the throttle percentage, engine load and torque should also have an impact on the estimation of fuel consumption.

### 4.4.3 Adding a tank lid state to the network

Another result was the large benefits that tank lid state information gave. An implementation of the signal to the FlexRay could have large benefits and would make it possible to detect online refuelling efficiently. Otherwise it would be interesting to investigate other techniques to detect online refuelling.

Even with the lid state present detection of offline and online refuelling can be difficult. The solution presented in this thesis involves an angle model, the last measured value and the state of the car. It is still a rather unexplored problem, and further investigation about the problem would be beneficial.

### 4.4.4 Implementation of angle logic

A conclusion that has been drawn from this thesis is that including either angle or acceleration signals in fuel level predictions have major advantages. It is therefore beneficial to investigate how these features can be implemented with current filters used in the cars. Large changes in software can take long time to implement. A simple change that can be implemented is the logic for offline refuel detection. By adding angles to the detection, it is possible to avoid false refuel detections.

The angle model presented in this thesis is based on an experiment. It may be possible to construct equivalent angle models from simulations. It will then be easier and cheaper to make specific models for each tank size.

The acceleration data could be used instead of using the angle data. The dynamics are captured by both signals, but the acceleration data is sent with a higher frequency on the FlexRay bus.

### 4.4.5 Future evaluation

One of the large difficulties in this thesis has been to evaluate the estimators, since no true value was available. A way to overcome this problem is to install a sensor with better precision inside a test tank. For example a ultrasound sensor could be installed. The high precision sensor could then be used to benchmark the behaviour of the filters.

# 5

## Conclusion

The aim of this thesis was to investigate what filtering methods that provide a sufficient and robust fuel level estimation. This was done by first examining different disturbances, then constructing a model and finally comparing different filter structures.

Different problems related to fuel level estimation were investigated. The inherent problems of fuel level estimation are based on a few types of disturbances. These disturbances include liquid slosh as this makes fuel readings very noisy. The noise properties also change as a function of acceleration and total volume of fuel. The signals read from the fuel level sensor and its translation to volume in litres is designed based on one fuel tank. Fuel tanks can deviate in size and therefore this translation is not always accurate. Inclined parking gives a biased fuel level reading and is therefore another factor that disturbs read fuel levels. All of these factors have been considered in the design of the filters.

Angular orientation has been considered a major factor that disturbed fuel level readings. Therefore a lab based experiment was setup to find a relationship between fuel level readings and angular orientation. This experiment had a saddle type tank tilted at various angles with various petrol volume. This experiment showed that the relationship between angles and fuel level readings could be modelled piece-wise linearly or as an adaptable model.

Variants of Kalman filters, a  $\mathcal{H}_\infty$  filter, particle filter and a RLS filter have all been compared with each other. There were two different types of Kalman filters, one with a simple model and one with a complex model. The complex model used angular orientation. The  $\mathcal{H}_\infty$  and particle filter used the same simple model. The RLS filter used a ARX based model by having longitudinal and lateral acceleration. The Kalman filter with a complex model along with the RLS filter were chosen to be further developed on.

Results showed that both the finalised filters behaved sufficient in the situations tested. However it was concluded that the Kalman filter was generally smoother and more tunable, faster in its convergence to zero fuel. The RLS filter was more noisy and was slower in its convergence to zero. It also followed fuel level trends more, which were not always necessarily better. It was however better in its way of handling angular offset readings from the fuel level sensor. In conclusion the better filter would be the filter that combines the best aspects of both the filters.

# Bibliography

- [1] Jonas Eklund, Rickard Kreuger.
- [2] Wikipedia: *Rpy angles of cars*, 2008. [https://upload.wikimedia.org/wikipedia/commons/f/f5/RPY\\_angles\\_of\\_cars.png](https://upload.wikimedia.org/wikipedia/commons/f/f5/RPY_angles_of_cars.png).
- [3] Volvo Car Corporation: *Internal documents*, 2017.
- [4] D’Alessandro, Vincenzo: *Modeling of tank vehicle dynamics by fluid sloshing coupled simulation*. 2012.
- [5] Volvo Car Corporation: *An introduction to fuel system*, May 2017.
- [6] *National instruments: Flexray automotive communication bus overview*. <http://www.ni.com/white-paper/3352/en/>. Accessed: 2018-05-09.
- [7] Yan Li, Li Yuxing, Qihui Hu Wuchang Wang Bin Xie Xichong Yu: *Sloshing resistance and gas–liquid distribution performance in the entrance of lng plate-fin heat exchangers*. 82, May 2015.
- [8] Lennart Ljung: *Black-box models from input-output measurements*. 1:138 – 146 vol.1, June 2001.
- [9] Lennart Ljung: *System identification - theory for the user*.
- [10] Ramser Faragher: *Understanding the basis of the Kalman filter via i simple and intuitive derivation*. IEEE Signal Processing Magazine, pages 128–132, September 2012.
- [11] L. Kleeman: *Understanding and applying Kalman filtering*. Master’s thesis, Monash University.
- [12] Urban Forssell: *On  $\mathcal{H}_\infty$  and  $H_2$  optimal estimation*, 1996.
- [13] Simon, Dan: *From here to infinity*.
- [14] J. Seo: *An extended robust  $h$  infinity filter for nonlinear uncertain systems with constraints*. Decision and Control.
- [15] M. J. Grimble, A. E. Sayed: *Solution of the  $\mathcal{H}_\infty$  optimal linear filtering problem for discrete-time systems*, volume 38. IEEE Trans. on Acoustics Speech and Signal Proc., 1990.
- [16] Lisa Turner: *An introduction to particle filtering*, 2013.
- [17] Roland Lamberti, Yohan Peletin, François Desbouvries: *Independent resampling sequential monte carlo algorithms*. IEEE Transactions on Signal Processing, 65(20), October 2017.
- [18] Tomas McKelvey: *Lectures notes in Applied Signal Processing*. Chalmers University of Technology, February 2014.
- [19] John A Rise: *Mathematical Statistics and Data Analysis*. 2007.
- [20] Julien Frère, François Hug: *Between-subject variability of muscle synergies during a complex motor skill*. 6, December 2012.

- [21] M.D. Bradley, E. CopeLand: *Standard deviation. a practical means for the measurement and control of the precision of clinical laboratory determinations.* American Journal of Clinical Pathology, 27(20), May 1957.
- [22] Paolo Frasconi: *Machine Learning and Knowledge Discovery in Databases*, volume 2. The Springer Nature, September 2016.
- [23] Louise Hagman: *Impact of parameters on fuel level indication.* Master thesis, Lund University, Department of Chemical Engineering, June 2017.
- [24] Claudiu C. Remsing: *Lecture Notes - Linear Control.* RHODES UNIVERSITY, 2006.
- [25] Huibert Kwakernaak, Raphael Sivan: *Linear Optimal Control Systems.* Wiley-Interscience, a Division of John Wiley & Sons, Inc., 1972.
- [26] Ben Southall, Bernard F. Buxton, John A. Marchant . January 1998.
- [27] Volvo Car Corporation : *Ägarmanual online - xc60.* <https://support.volvocars.com/se/cars/pages/owners-manual.aspx?mc=y413&my=2017&sw=16w17&article=645be458f78dfe38c0a801e80158dabc>, May 2018.
- [28] Franco Maloberti: *Data Converters.* Springery, 2007.
- [29] Balázs Kulcsár: *Lecture Notes - Linear Control System Design (SSY285) - Frequency domain and robustness.* Chalmers University of Technology, 2017.
- [30] Sangjun Park, Hesham Rakha: *Energy and environmental impacts of roadway grades*, 2005.
- [31] Ahmet Gürkan Capraz, Pinar Özel, Mehmet Sevkli Ömer Faruk Beyca: *Fuel consumption models applied to automobiles using real-time data: A comparison of statistical models*, 2016.

# A

## Measurement instruments

This chapter describes the measurement instruments used in the experiment described in Section 2.5. The experiment had the aim to measure the fuel displacement while changing the angle. The measurement tools used were a computer with required software and a measurement tool by the name of m-sense. This measurement tool had 4 input readings and reads an analogue voltage signal. The sampling time is set through the software on the computer.

A LG G6 telephone was used to capture angular orientation of the tank. This phone outputs an angle with the help of gyroscopes, a magnetometer and an accelerometer. The resolution of this angle measurement is up to one micro degree.

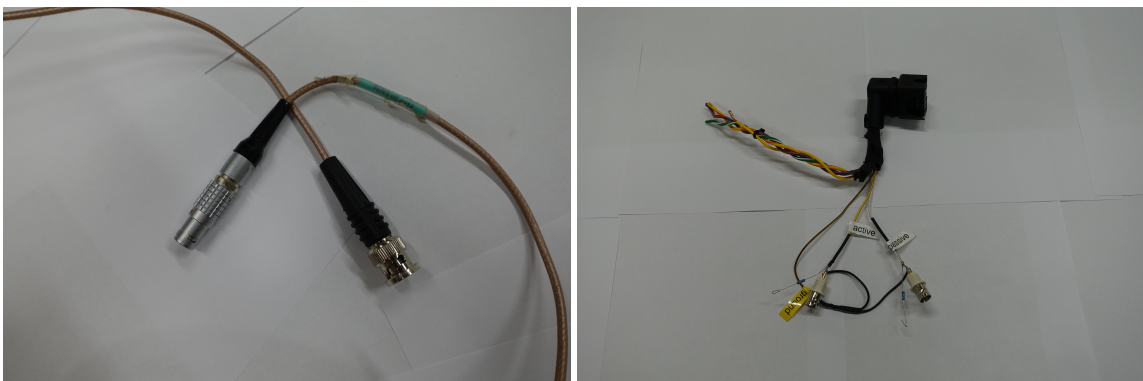
The second IMU unit could capture orientation but will only output a voltage. The settings of the device are unknown. Software for this sensor was also unavailable. Accuracy of the device is also unknown. The device is known as the 3DXM orientation sensor.

There were in total of four power supplies used. These power supplies could keep a constant DC voltage output and were called CPX400S SA SP. This power supply can keep the voltage constant within 0.3%.

The last remaining power supply is a constant output 12 Volt source.

### A.1 Cables

Cables that connect to the m-sense sensor are of BNC female connectors.



(a) A BNC female to m-sense port cable (b) A modified fuel pump cable

**Figure A.1:** Image a is a cable that connects to the m-sense sensor as well as the male BNC connectors on image b

Another important cable is a modified cable that is connected to the fuel tank. This cable is wired in such a way that the cable connects to the tank via a out BNC male, that measure the fuel level from the left and right side of the tank. These two BNC cables share the same Ground. This BNC cable has a resistor soldered onto the measuring port of the BNC.

There were 4 modified power cables that connects the power supply to the variable resistor circuits via a test pin hook.

Two resistors of 1000 ohm were used with an uncertainty of 1 percent.

A flask was used to measure the amount of fuel that went into the tank. The resolution on the flask is within  $\pm 10$  ml

## A.2 Inertial Measurement Unit

Two orientation sensors are used within this experiment. One is a advanced Inertial Measurement Unit (IMU), by the name 3DXM orientation sensor, however its settings are unchangeable since there is no available software for interfacing with the device. So far it is believed only the accelerometer provides a orientation signal.

The second sensor used is a sensor within the smart phone LG G6 that combines a magnetometer, gyroscope and a accelerometer to compute angular orientation.

The 3DXM sensor is however synced up with data in regards to fuel level measurements whilst the phone is not. Therefore the 3DXM sensor will be used to help to determine at which time-stamp the orientation signals of the phone are influencing fuel tank readings.

The 3DXM sensor can also be used to establish a relationship between angles and fuel volume reading errors, however the sensor is noisy therefore the LG G6 is preferred.

# B

## Measuring the resistance of the resistor cards in the tank

It is only possible to measure voltages with the measurement tools provided. This means that a system must be made such that the resistance of the variable resistors in the tank is measured through a change in voltage. The way to do this is to connect a known resistor in series with the resistor card circuit and measure the voltage drop across the known resistor.

The measurement computer is firstly connected to the m-sense sensor via a cable interface. The sensor is powered with a power supply of 5 volts. Each variable resistor circuit within the tank is powered by independent power supplies in order to keep voltage drops for each circuit independent of each other.

In theory if the total voltage is kept constant then it is possible to compute the resistance of the variable resistor using Ohms law.

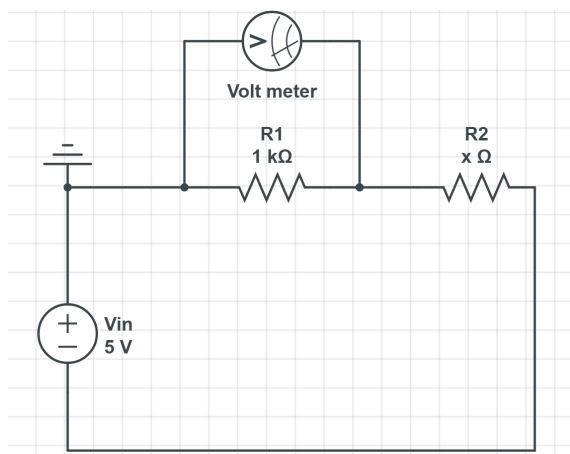


**Figure B.1:** The measurement circuit with a 5 volt voltage source. Measurement is done across the known resistor as seen by the voltage meter

Firstly, Ohms law states that,

$$\begin{aligned}
 V_{total} &= I_{total}R_{total} \quad ,\text{where:} \\
 \sum_{i=1}^n V_i &= V_{total} \\
 \sum_{i=1}^n I_i &= I_{total} \\
 \sum_{i=1}^n R_i &= R_{total}
 \end{aligned}
 \tag{B.1}$$

Which can be rewritten as:

$$\begin{aligned}
 V_{total} &= V_1 + V_2 \\
 V_2 &= V_{total} - V_1 \\
 R_2 I_{total} &= V_{total} - V_1
 \end{aligned}
 \tag{B.2}$$

In order to remove current from the equation in B.1 the relationship below can be used.

$$I_{total} = \frac{V_{total}}{R_1 + R_2}
 \tag{B.3}$$

Replacing equation B.2 with B.3 results in the equation below.

$$\begin{aligned}
 \frac{V_{total}}{R_1 + R_2} R_2 &= V_{total} - V_1 \\
 \frac{V_1 R_1}{V_{total} - V_1} - R_2 &= 0
 \end{aligned}
 \tag{B.4}$$

This yields the final equation which maps the voltage read across the known resistor to the resistance of the variable resistor.

$$\frac{V_1 R_1}{V_{total} - V_1} = R_2
 \tag{B.5}$$